POLYTECHNIQUE MONTRÉAL
TECHNOLOGICAL UNIVERSITY

NON-PLANAR MULTINOZZLE ADDITIVE MANUFACTURING OF THERMOSET COMPOSITES

Twenty-third International Conference on Composite Materials (ICCM23)

ICCM 23 BELFAST 2023

Jean-François Chauvette, PhD

Laboratory of multiscale mechanics

30th July – 4th August, 2023

SAFRAN | NSERC CRSNG | INNOVATION.CA — CANADA FOUNDATION FOR INNOVATION / FONDATION CANADIENNE POUR L'INNOVATION | Chaires de recherche du Canada | CREPEC — Research Center for High Performance Polymer and Composite Systems

MOTIVATION

- Additive Manufacturing (AM) / 3D printing in the aerospace industry

Lighter parts | Reduction of material losses | Flexibility for complex geometry

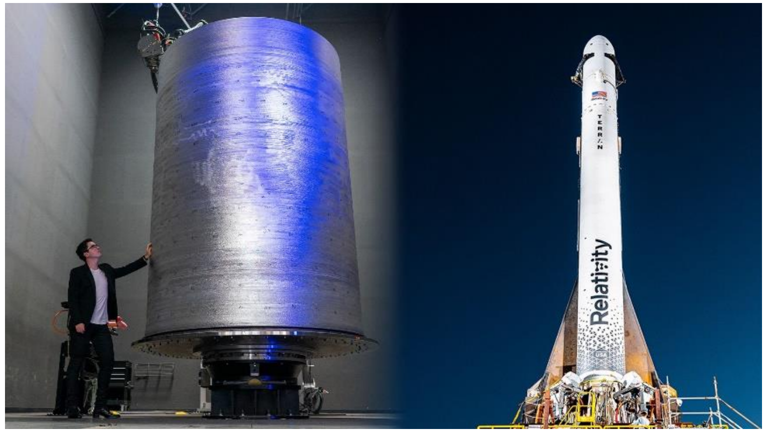

Relativity Space 3D-printed Terran 1 rocket (wsj.com, 2023)

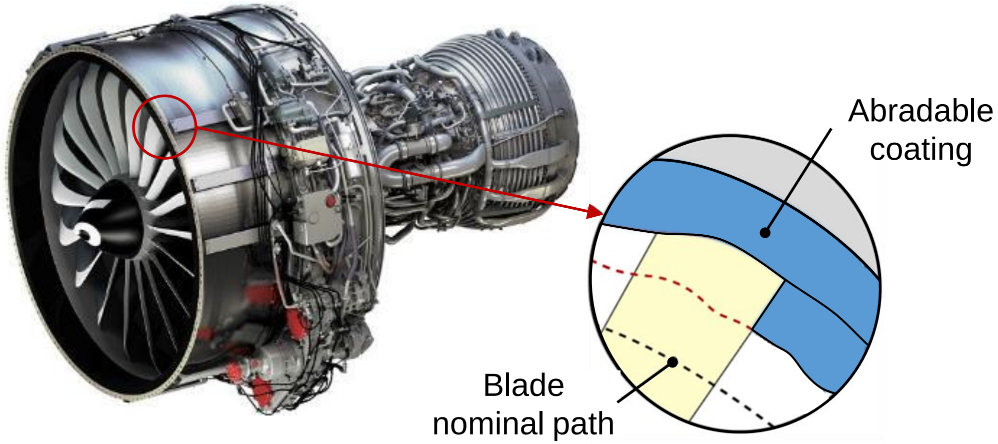

Aircraft gas turbine engine (www.safran-group.com)

- Investigation of AM for fabricating abradable thermosetting composite coatings
  - Multifunctional capability
  - ACARE (Advisory Council for Aviation Research and Innovation in Europe) standards[1]
    - 55% reduction of CO_2 emission by 2030 and net-zero by 2050
    - 65% reduction in perceived noise by 2050

1. https://www.acare4europe.org/acare-goals/

SELECTED ADDITIVE MANUFACTURING CONCEPTS

- Layer-by-layer fabrication
- Direct Ink Writing (DIW)
  - Material extrusion technique
  - Viscoelastic inks, room temperature
  - Microscaffolds
    - Popular application for tissue engineering
    - Potential for sound absorption
  - Multinozzle printhead
- 6-axis robot for AM
  - Non-planar
  - Large-scale

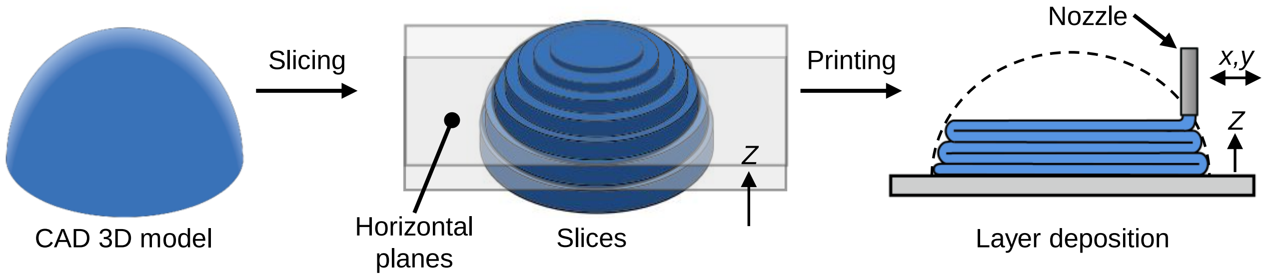

Schematics of layer-by-layer material extrusion (adapted from Nisja et al., 2021)

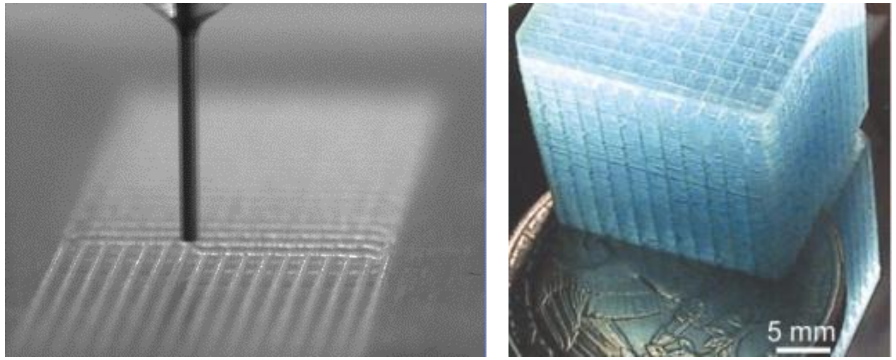

DIW of a microscaffold (Therriault et al., 2005)

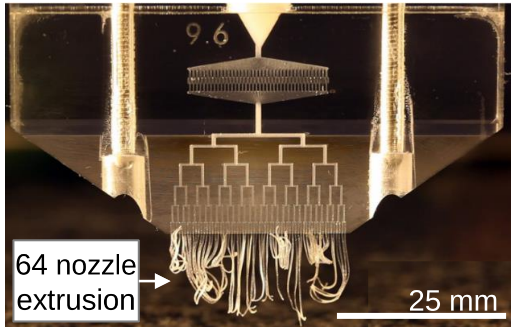

Multinozzle DIW (Kranz, 2013)

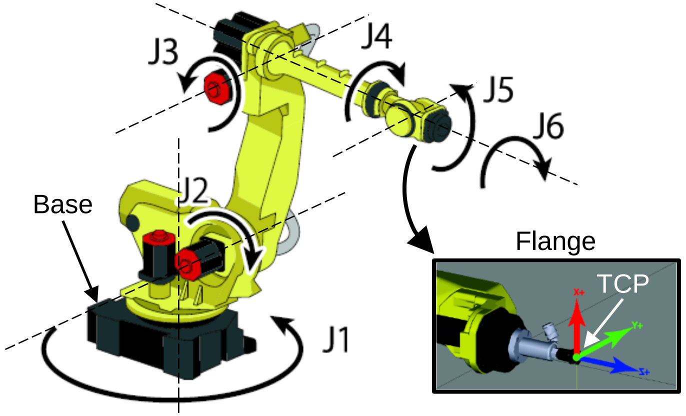

Schematic of 6-axis robot (Fanuc America Corporation, 2018)

3D-printed bridge (Striatus project, ETH Zürich, 2021)

PROBLEM IDENTIFICATION & OBJECTIVE

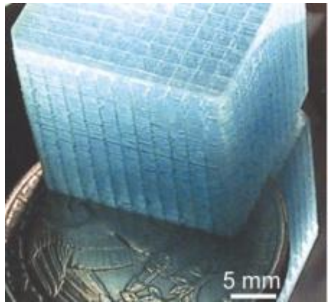

- Main challenges
  - DIW of thermosetting microscaffolds
    - **Small-scale** applications
  - 6-axis robots for large-scale AM
    - Mostly **single nozzle** non-planar AM
    - **Long printing times** with high resolution (*e.g.*, up to days).
  - Current multinozzle printhead technologies
    - Relatively **low flow rates** and low viscosity material.
    - No report of **non-planar multinozzle AM** with complete freedom of printhead orientation.

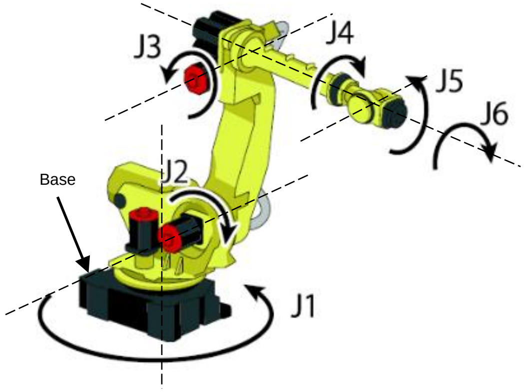

- General objective

> Develop a non-planar multinozzle AM approach using a 6-axis robot to achieve large-scale manufacturing of high-resolution thermosetting microscaffolds

6-AXIS ROBOT AM INFRASTRUCTURE

- AM workflow and experimental setup

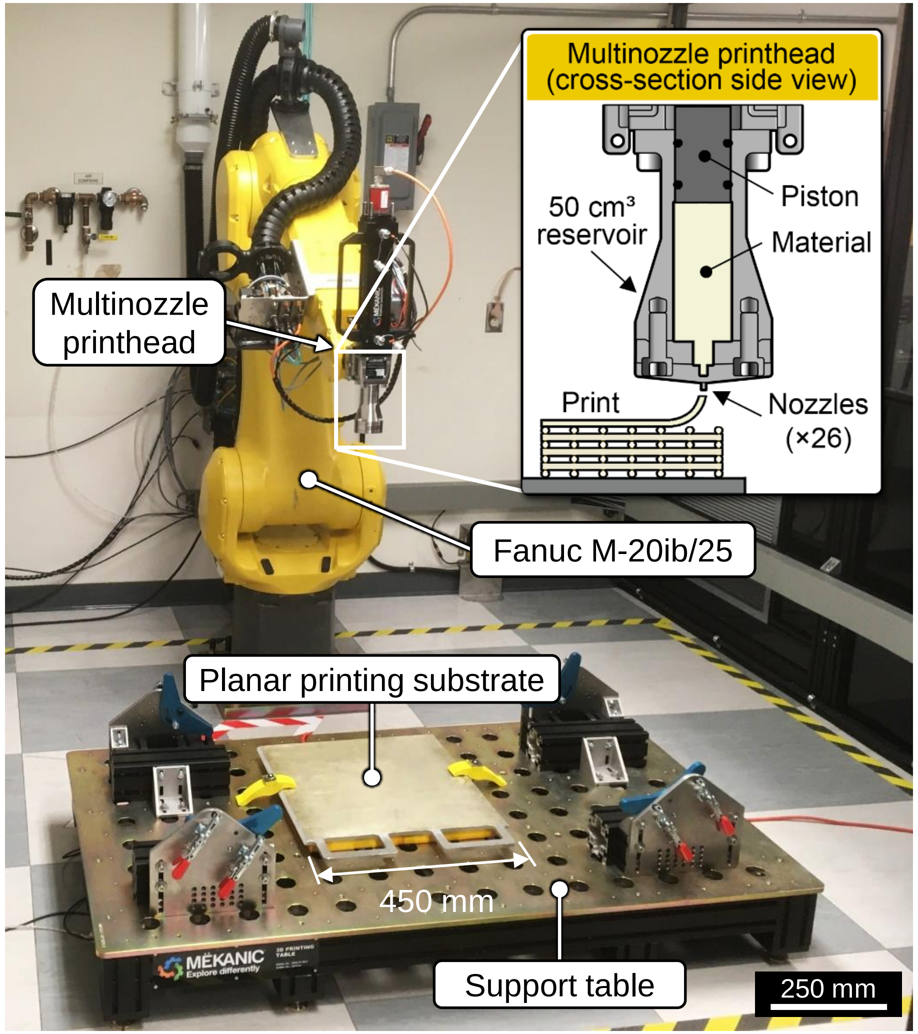

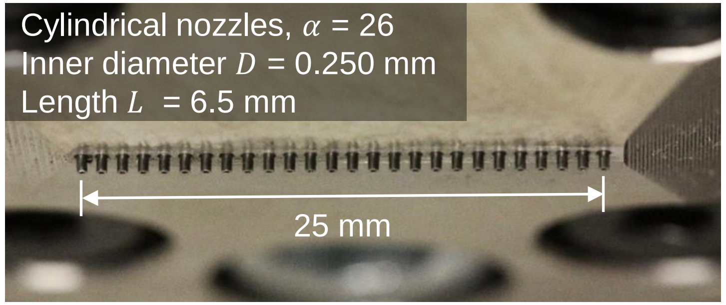

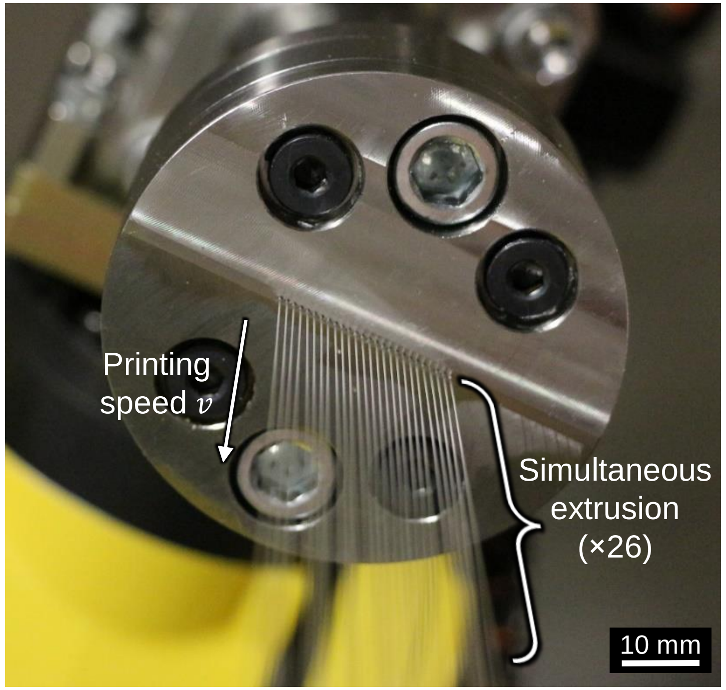

PLANAR PRINTING CASE STUDIES

- Pressure prediction : **Multinozzle Extrusion Prediction Model (MEPM)**
  - Predicting for printing speed v = 50 – 250 mm/s
  - ΔP recorded using Wika A-10 sensor + Labview

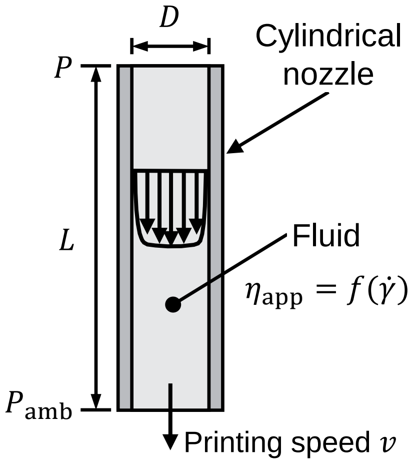

$\Delta P = P - P_{amb}$

(1) $\eta_{app,i} = K\,\dot{\gamma}_i^{\,n-1}$

(2) $R_i = \frac{128\,L\,\eta_{app,i}}{\pi\,D^4}\left(\frac{3+1/n}{4}\right)$

(3) $\Delta P = R_{eq}\sum_{i=1}^{\alpha} Q_i$

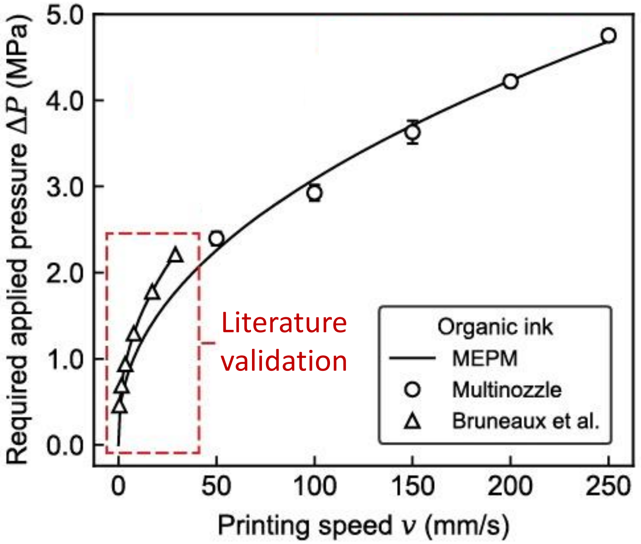

Case studies pressure prediction using organic ink

- Material : Organic ink[1]

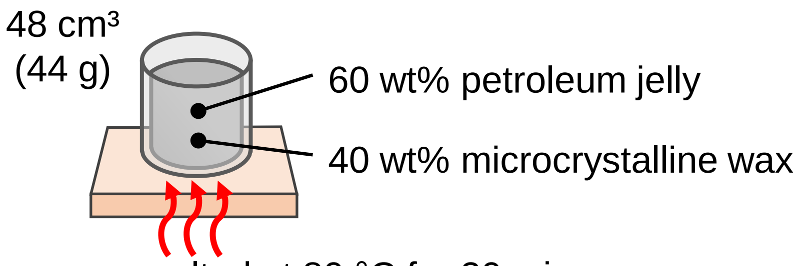

1. Therriault et al., Advanced Materials, 2005

PLANAR PRINTING CASE STUDIES

- High-speed printing of microscaffold network
  - Network of 9 × 15 microscaffolds (generated with each printing passes)
  - ΔP = 4.75 MPa, v **= 250 mm/s** (Q_{tot} = 319 mm³/s)

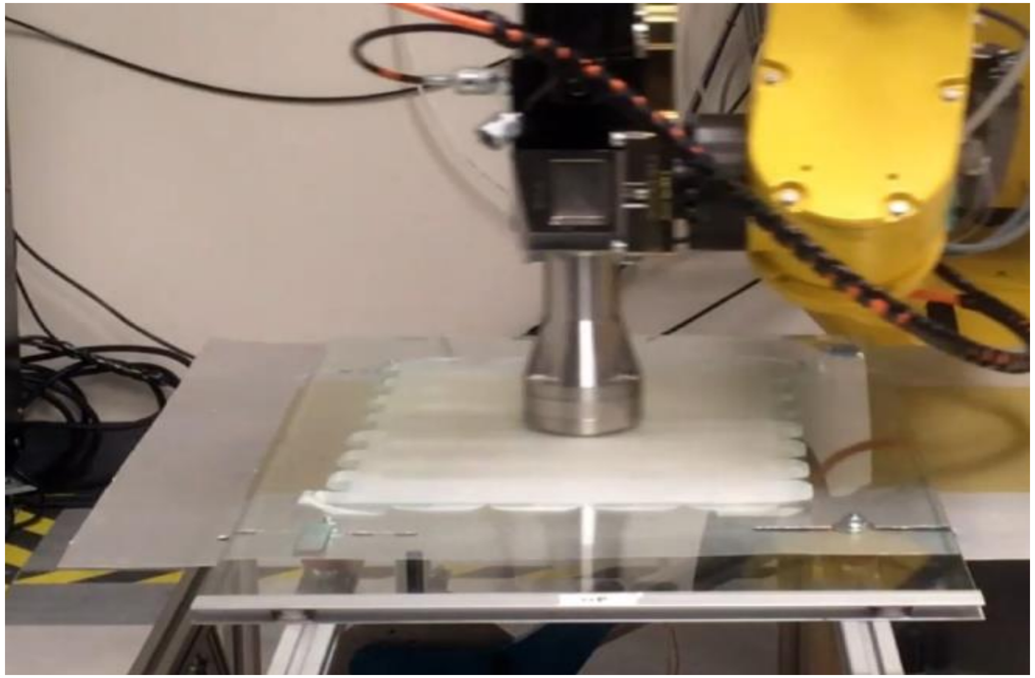

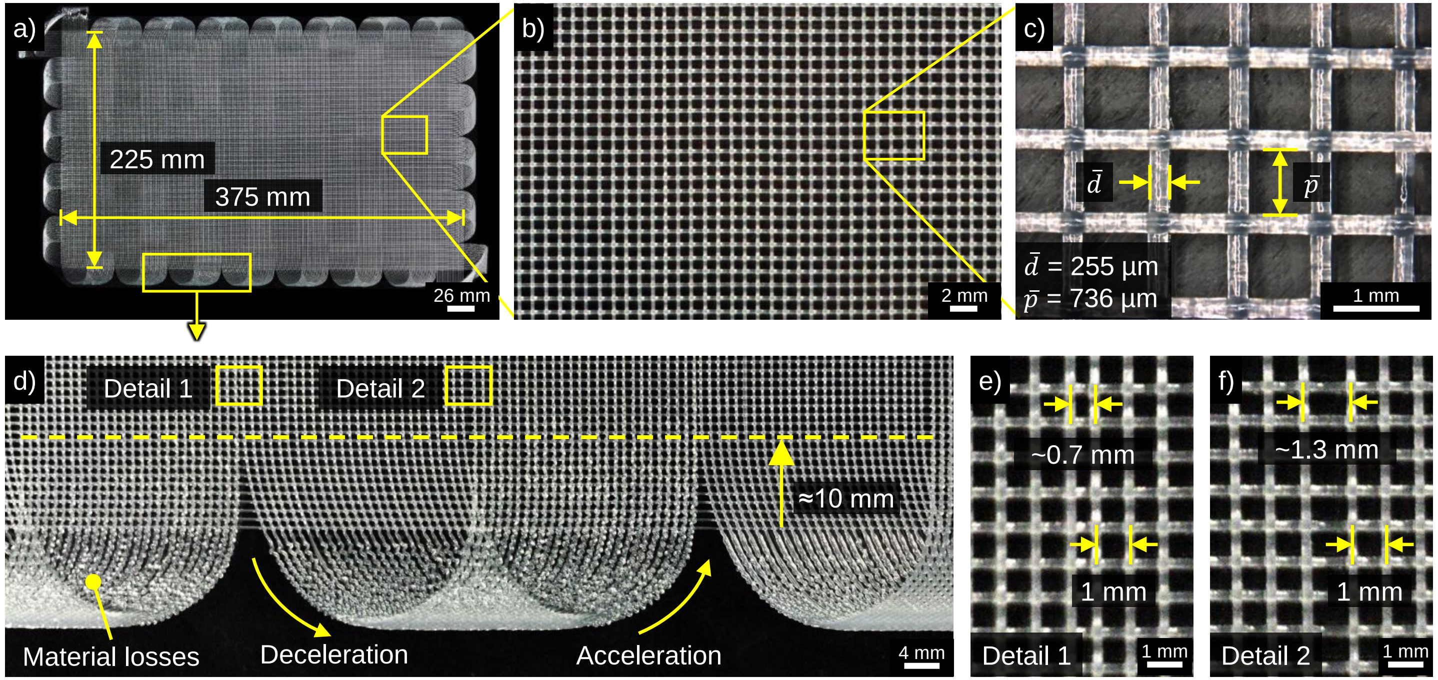

  - 5 layers (1 mm thick), 234 × 390 printed filaments
  - Printing time = **1 min 30 s** (vs. 41 min with single nozzle)
    - 3 times faster than previously published work for similar results[1]

1. S.J. Kranz, “Multinozzle Printheads for 3D Printing of Viscoelastic Inks”, University of Illinois at Urbana-Champaign

PLANAR PRINTING CASE STUDIES

- Thick partitioned microscaffold network
  - 3 × 3 network + walls
  - **50 layers** (10 mm), 78 × 78 filaments
  - ΔP = 2.40 MPa, v = 50 mm/s (Q_{tot} = 63.2 mm³/s)
  - t = 8 min 45 s

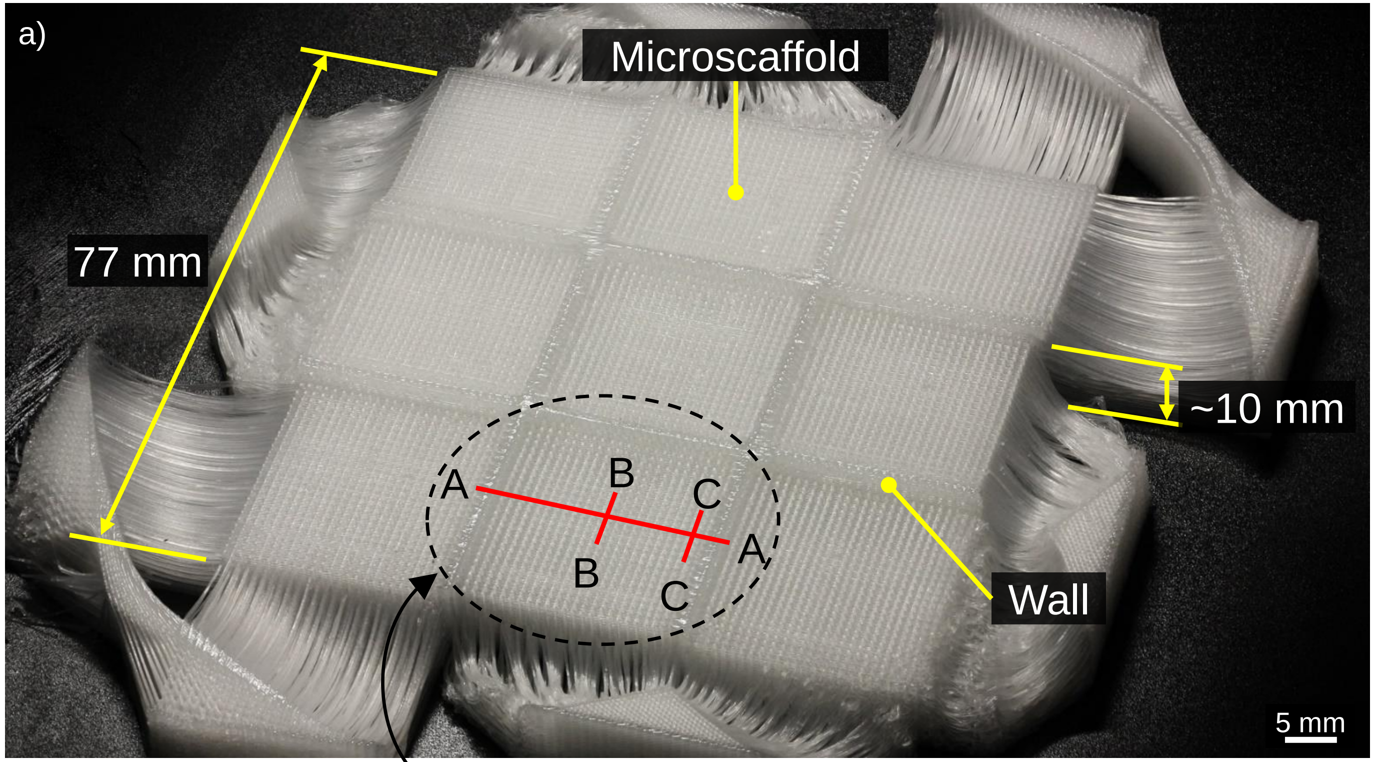

X-ray micro-CT scanned volume
(following epoxy encapsulation)

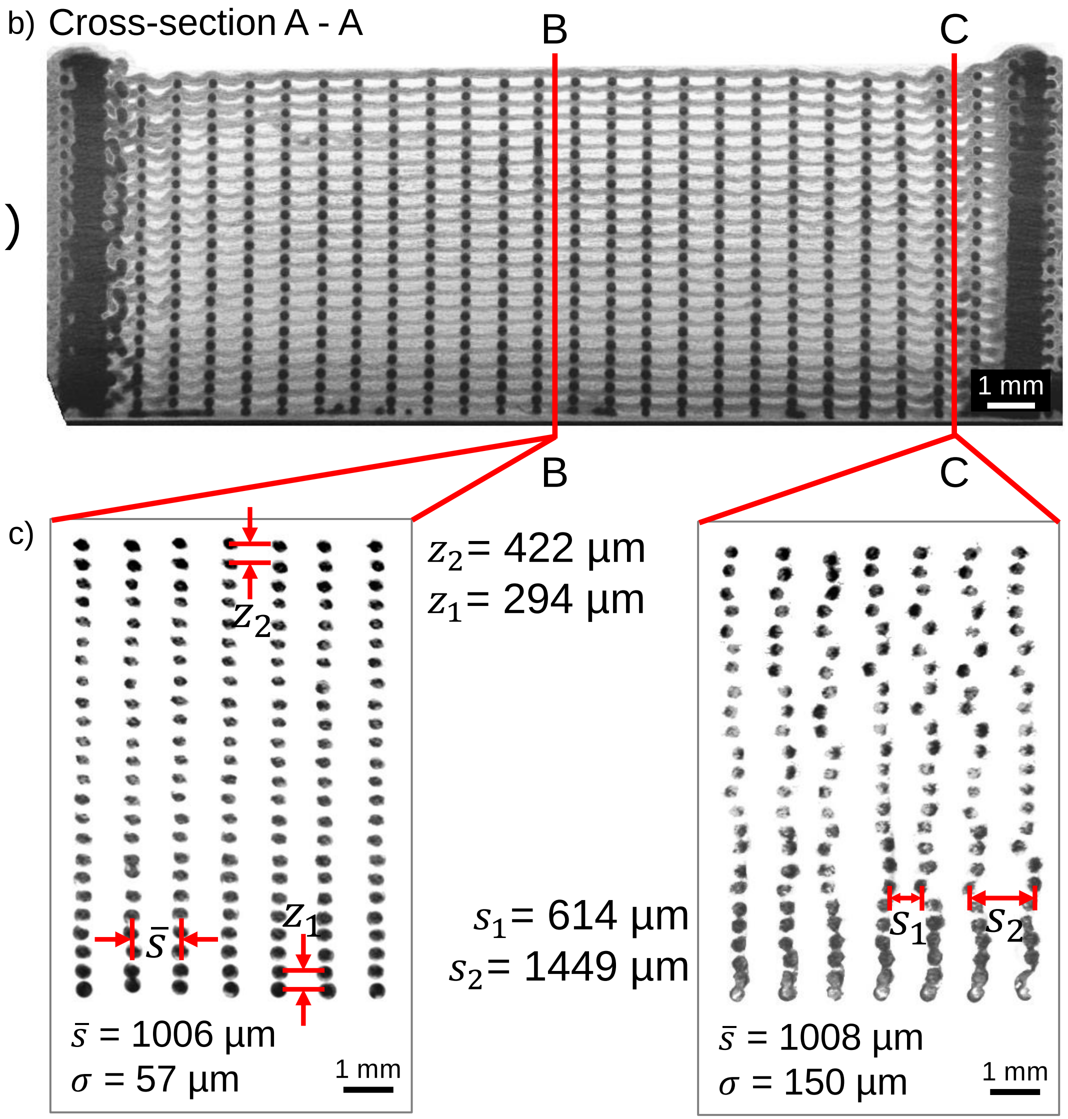

Cross-section B - B

Cross-section C - C

THERMOSETTING POLYMER MATERIAL

- Preparation and mixing[1]

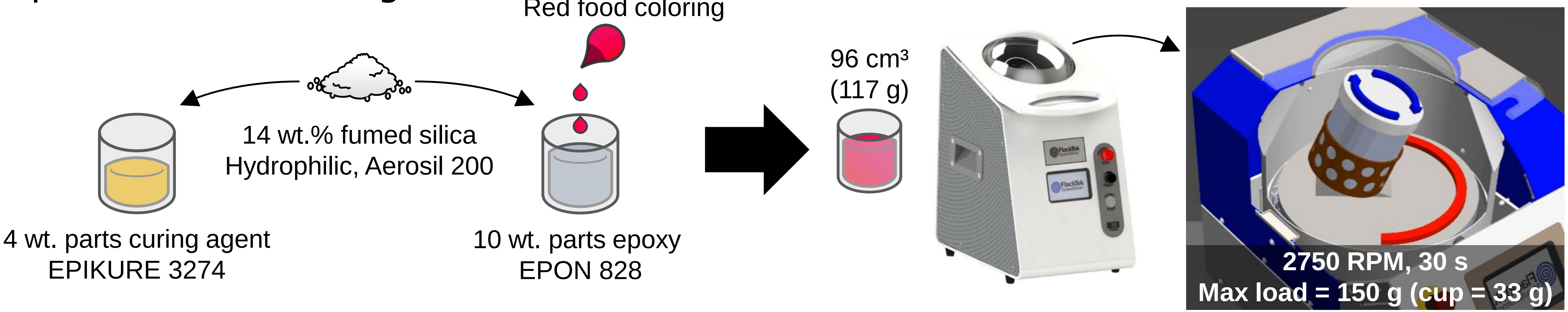

DAC 330-100 SE SpeedMixer

- Viscosity characterization
  - Shear-thinning behavior

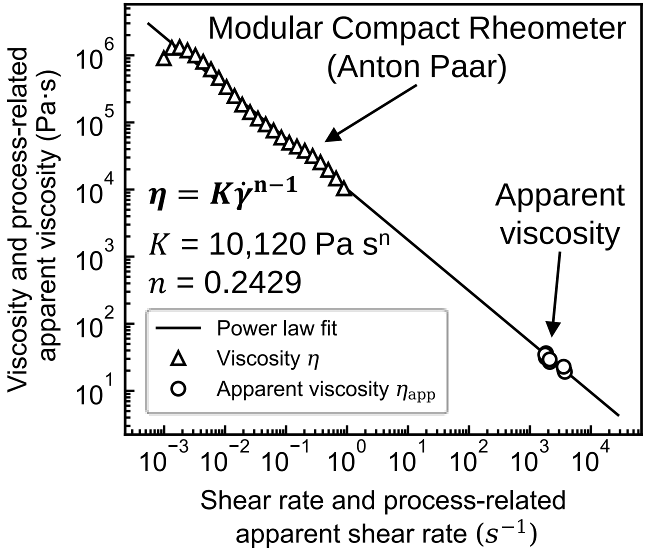

1. In collaboration with David Brzeski and Iee Lee Hia (FACMO research Chair)

NON-PLANAR MICROSCAFFOLD GENERATION

- Python program : **Multinozzle Toolpath Generator (MTG)**
  - Input = surface scan mesh, multinozzle config., network definition, printing parameters
  - Output = **non-planar multinozzle AM trajectory** for 6-axis robots
  - **Collision avoidance** between nozzles and substrate

Step 1 : NURBS parametrization

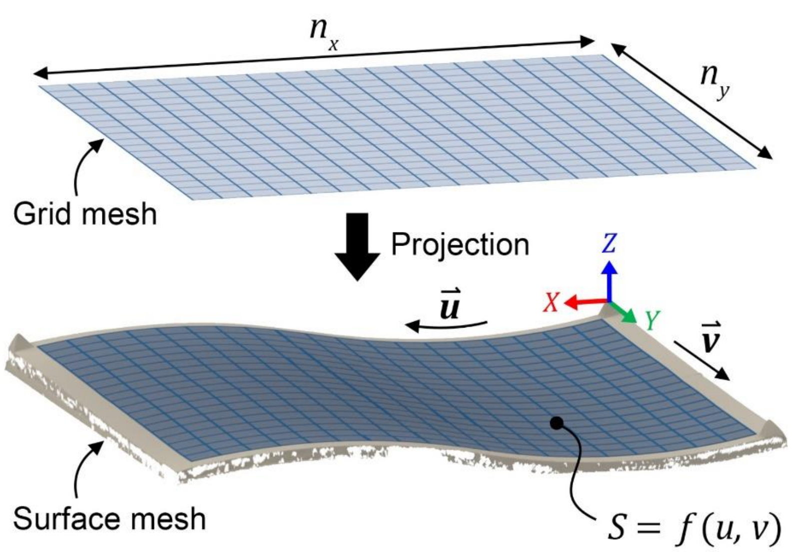

Step 2 : Toolpath generation + projection

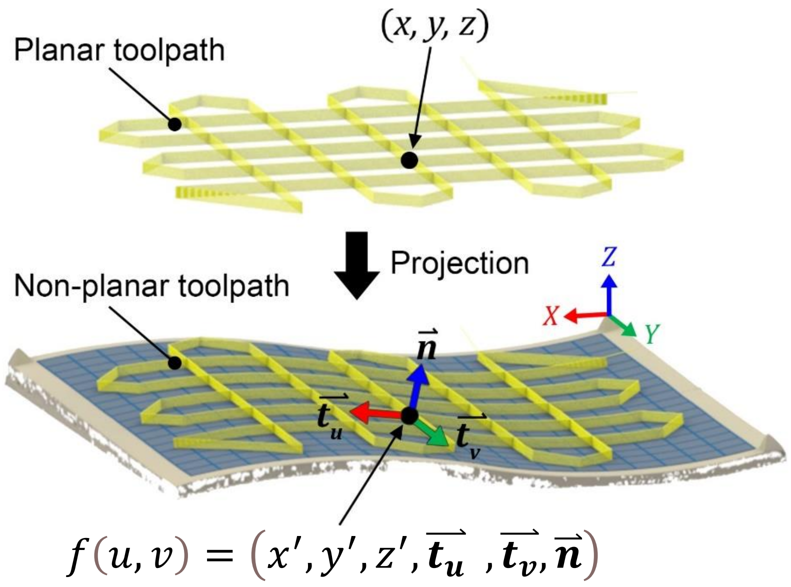

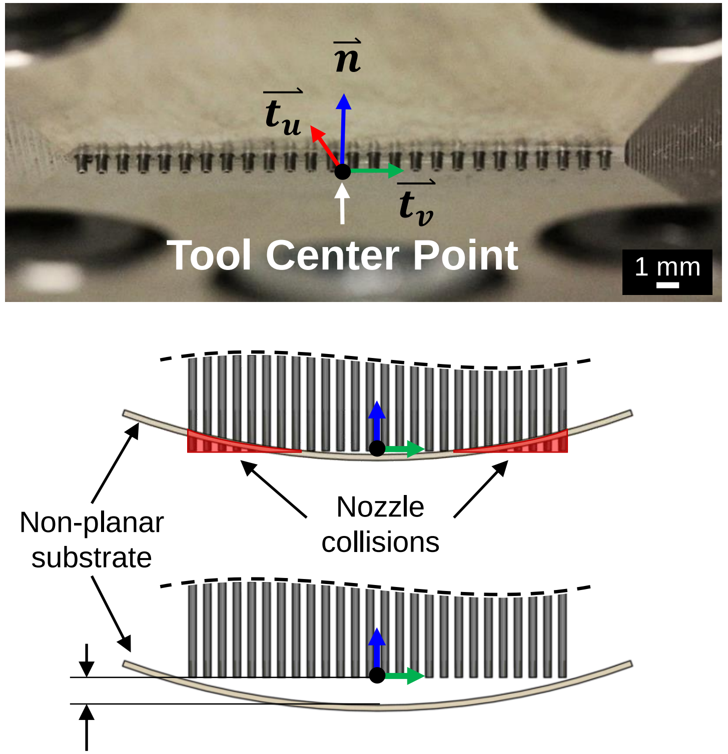

Found clearance
$\Delta z_{\max} = 24.2D$ (material specific)

NON-PLANAR MICROSCAFFOLD NETWORKS

- Surface of aircraft casing with double curvature
  - 5 × 15 network, 20 layers
  - v = 50 mm/s, ΔP = ~ 6 → 9 MPa
  - t = 20 min (vs. 8.5 h with single nozzle)

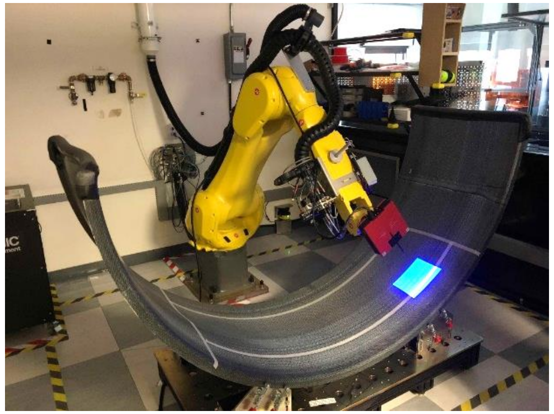

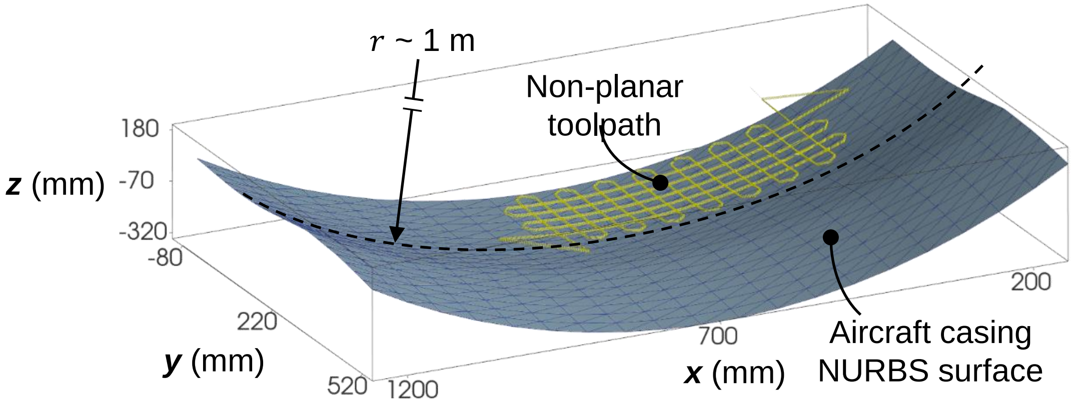

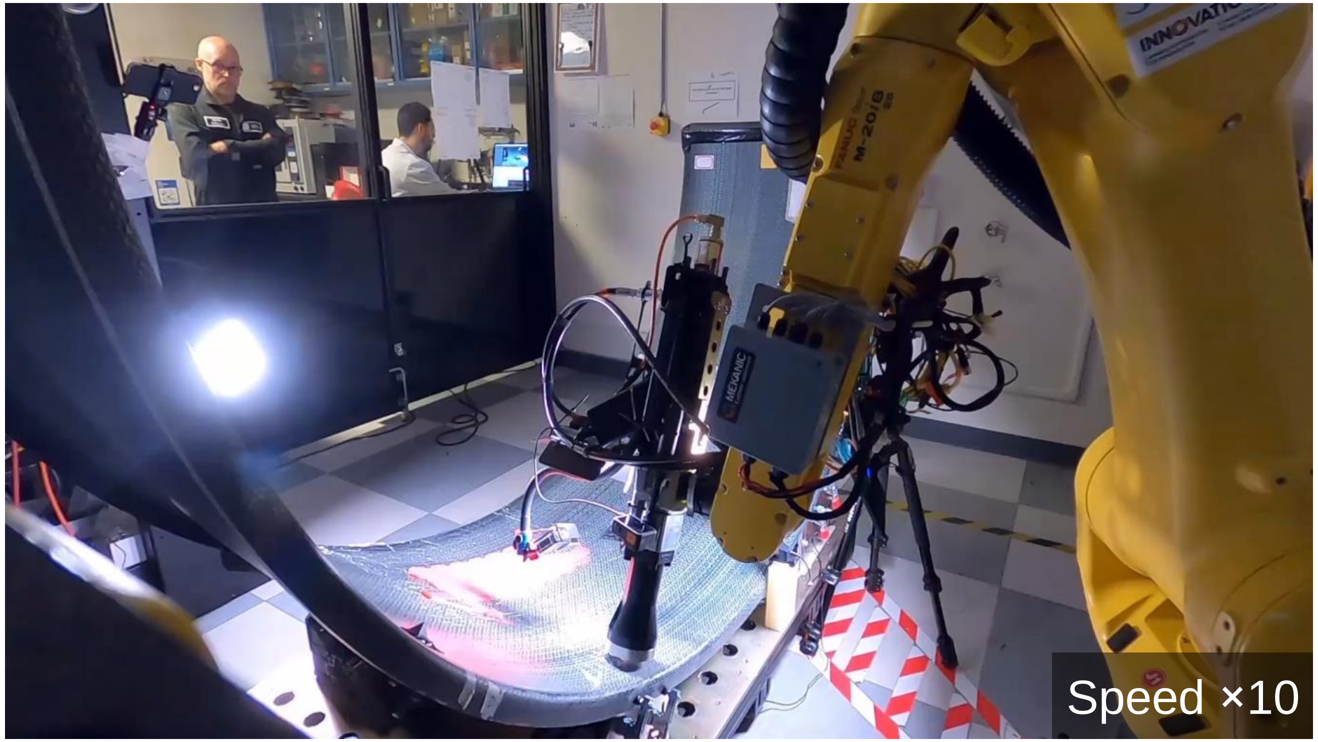

Timelapse video of non-planar multinozzle AM on aircraft casing

POLYTECHNIQUE MONTRÉAL UNIVERSITÉ D'INGÉNIERIE

NON-PLANAR MICROSCAFFOLD NETWORKS

LM²

- Surface of aircraft casing with double curvature

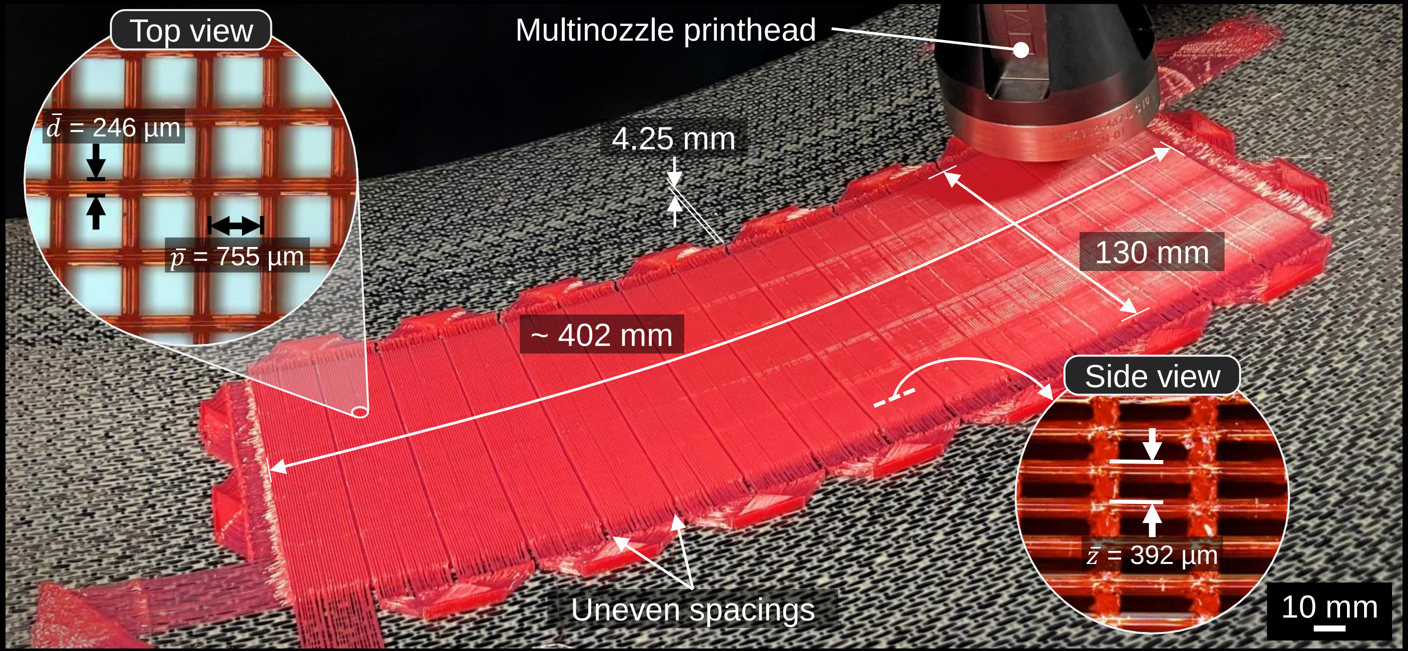

- Error $\bar{d}$ = 1.5 %
- Error $\bar{p}$ = 0.7 %
- Error $\bar{z}$ = 2.4 %

- Distance comparison with programmed toolpath[1]
  - Recorded toolpath using DigiMetrix Labview Fanuc library
    - 17,196 recorded points
    - 95% below saturation (0.020 mm)
    - Worst zone error = 15 µm (6 % of D)

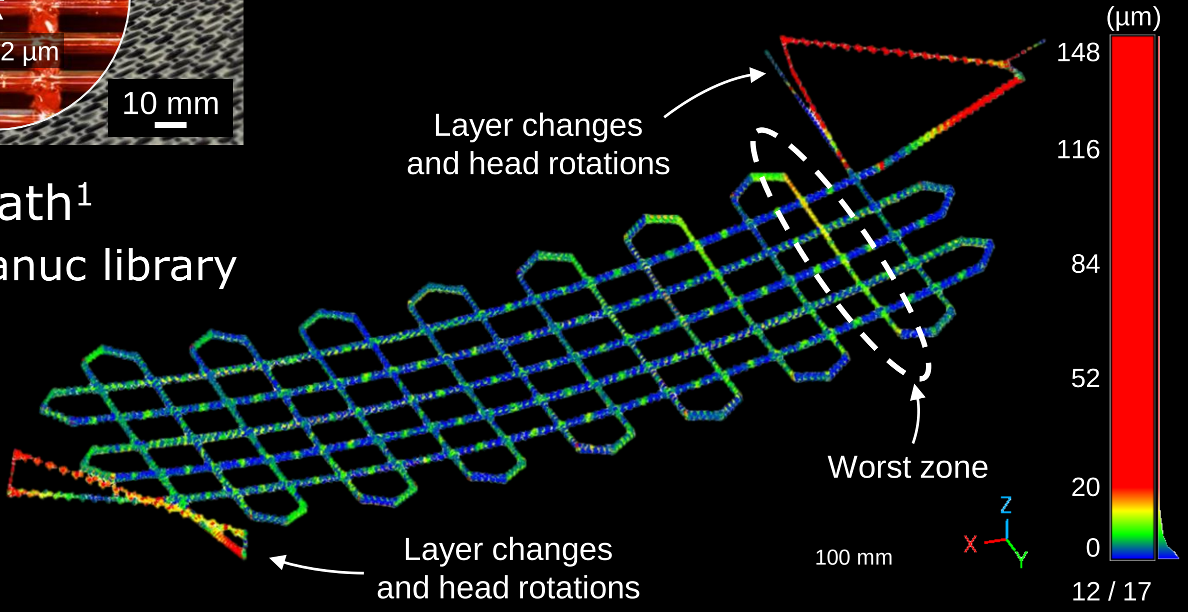

1. Using CloudCompare (https://www.danielgm.net/cc/)

POLYTECHNIQUE MONTRÉAL TECHNOLOGICAL UNIVERSITY

ABRADABLE THERMOSETTING COMPOSITE

LM²

- Preparation and mixing[1]

Modification of **commercial abradable resin** (EC-3524)

12 wt.% fumed silica
Hydrophobic, Cabot TS-720

SpeedMixer

~250 cm³ (320 g)

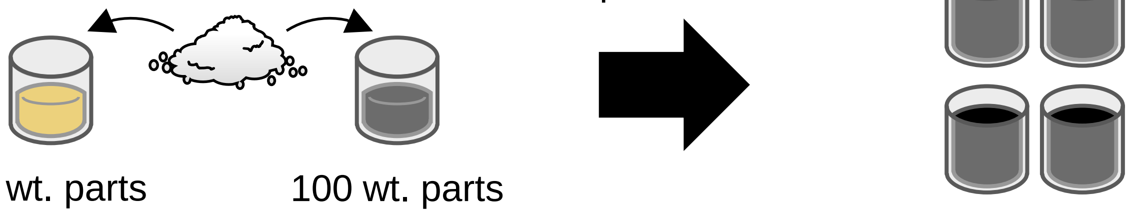

94 wt. parts curing agent "Part A"

100 wt. parts epoxy resin "Part B"

3D-printable highly viscous **abradable thermosetting composite**

- Viscosity characterization

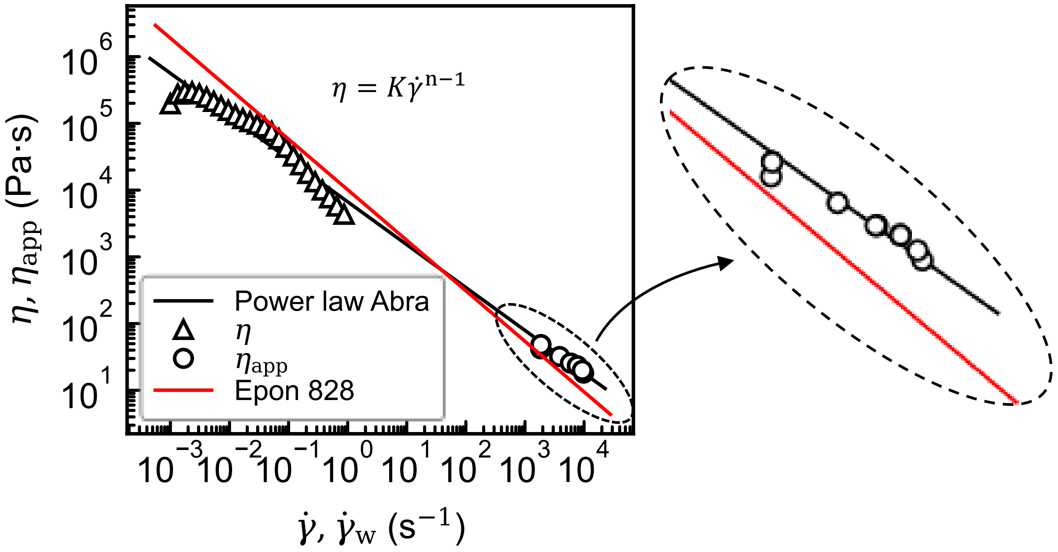

Abradable :
$K = 6{,}673$ Pa s^n
$n = 0.3578$

EPON 828 :
$K = 10{,}120$ Pa s^n
$n = 0.2429$

1. Brzeski et al., Additive Manufacturing, 2021

6-AXIS NON-PLANAR MULTIPROCESS AM

Step 1

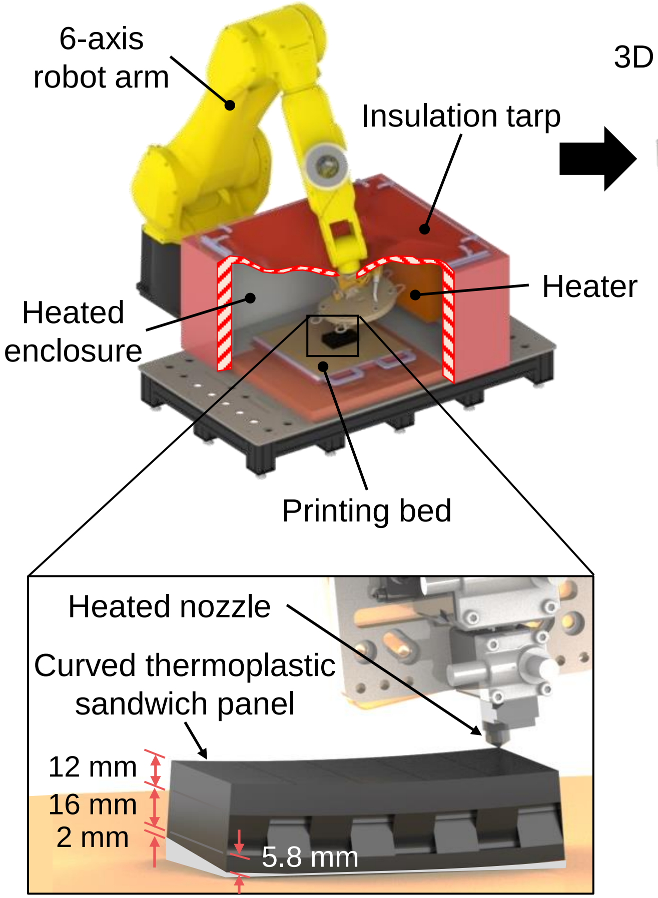

Non-planar FFF of thermoplastic sandwich panel (×4).
Nozzle **D = 0.4 mm**, **v = 15 mm/s**, **~ 60 h.**[1]

Step 2

Step 3

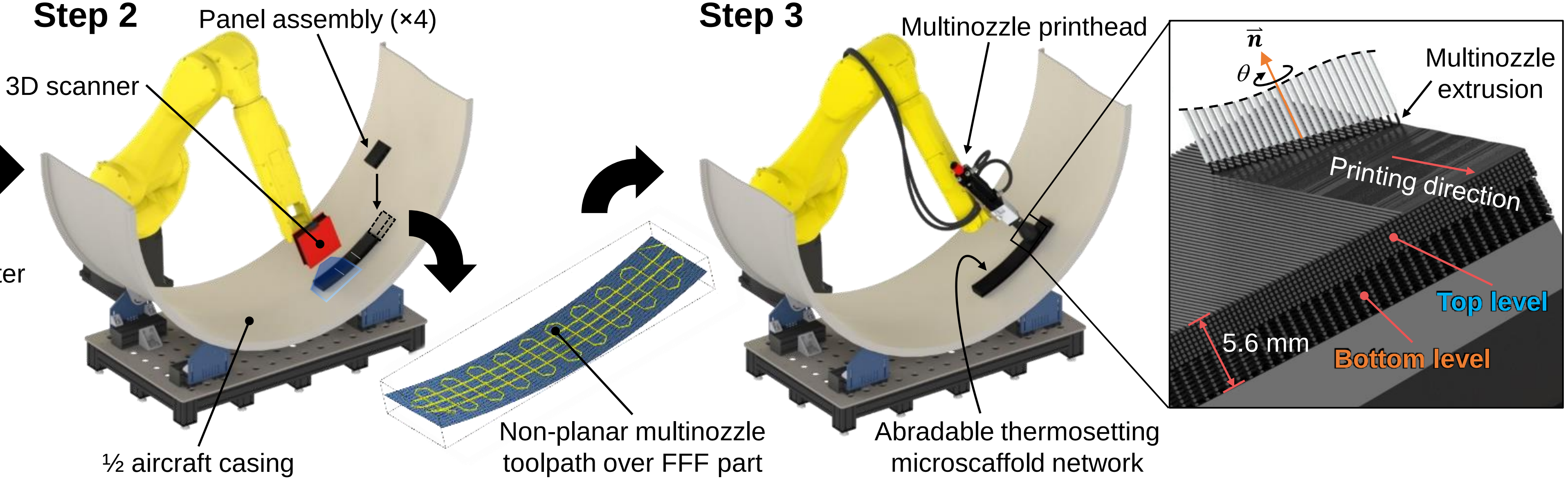

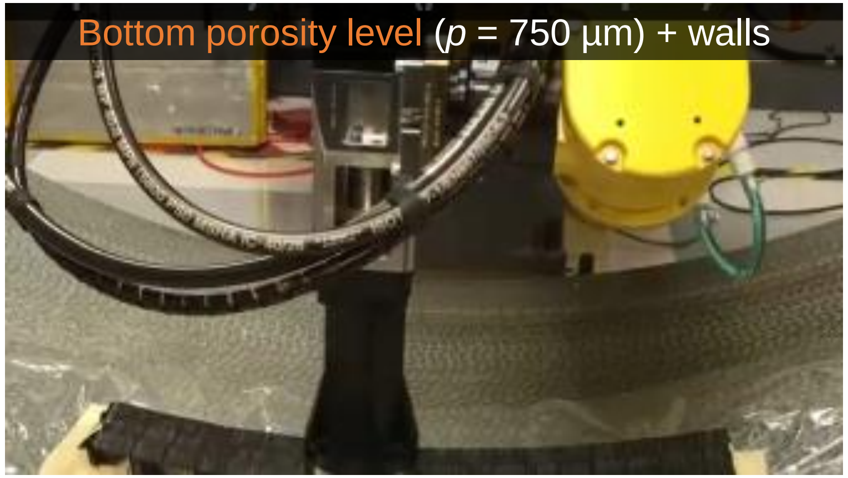

Non-planar multinozzle AM of 3D-printable abradable material on top of thermoplastic sandwich panel.
v = 50 mm/s, **ΔP = 9 → 18 MPa**, **t ~ 40 min**.

1. In collaboration with Juliette Pierre and Gabriel Chenier (FACMO research Chair)

6-AXIS NON-PLANAR MULTIPROCESS AM

- Aircraft component demonstrator
  - Bottom level : 3 × 19 network
    - 16 layers, p = 750 µm (3.2 % error)
  - Top level : 7 × 45 network
    - 14 layers, p = 184 µm (4.3 % error)
  - t ~ 40 min vs. ~ 20h with single nozzle
  - 1/12 circumference (proof of concept)
  - **Multifunctional (abradable + acoustic)**

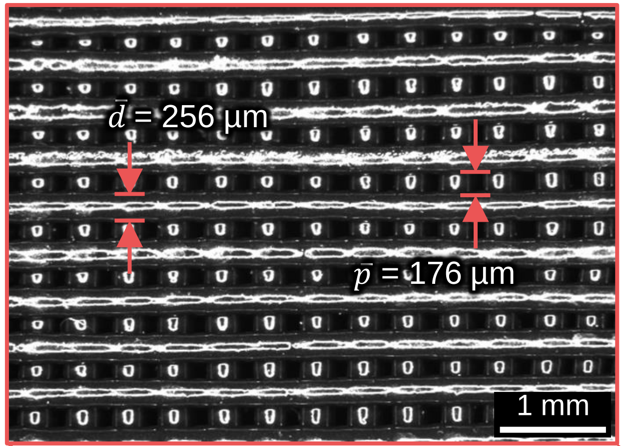

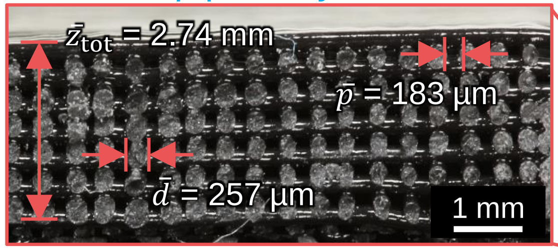

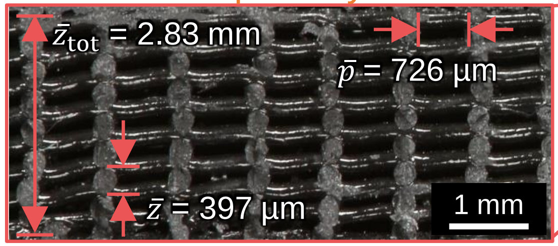

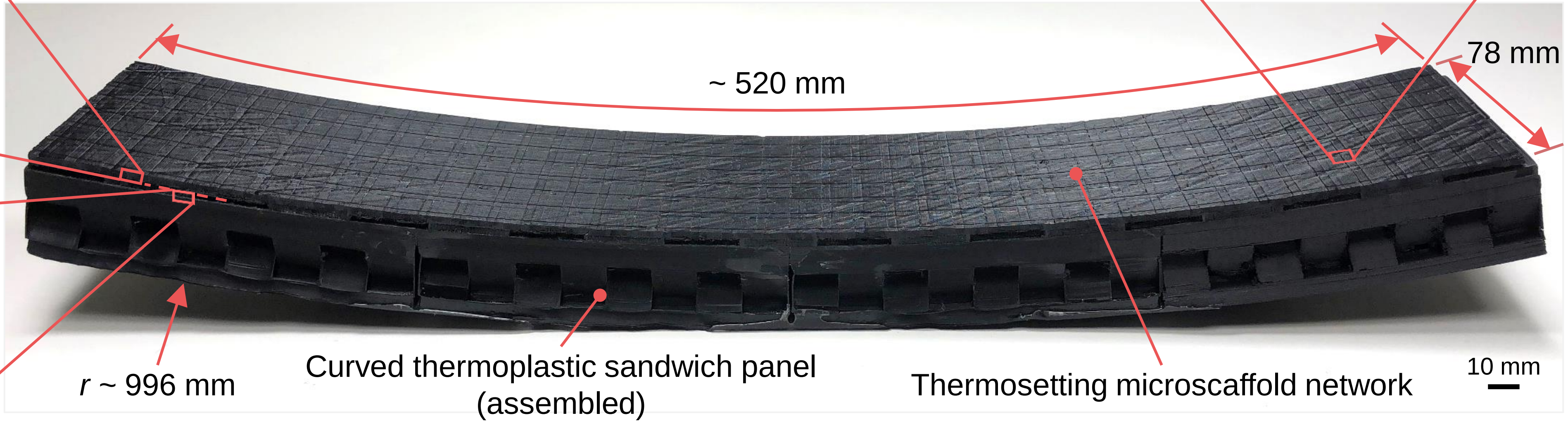

1. In collaboration with Juliette Pierre (FACMO research Chair)

CONCLUSION

Develop a non-planar multinozzle AM approach using a 6-axis robot to achieve large-scale manufacturing of high-resolution thermosetting microscaffolds

1. Investigate high-speed multinozzle additive manufacturing

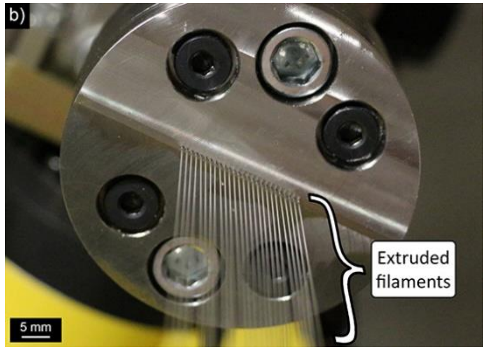

https://doi.org/10.1016/j.addma.2021.102294

- Open source Multinozzle Extrusion Prediction Model (MEPM)[1]
- ΔP prediction error = 3 %
- v = 250 mm/s (3× faster than literature)

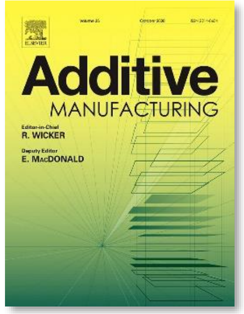

2. Expand the development of non-planar multinozzle additive manufacturing

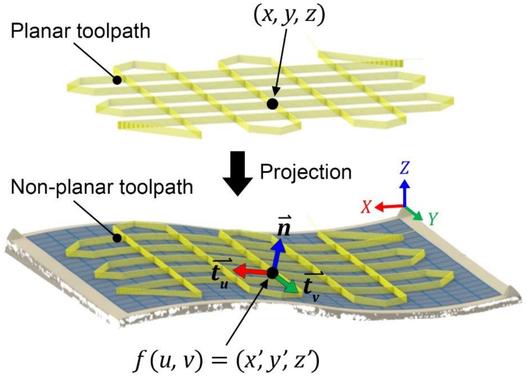

https://doi.org/10.1016/j.compositesb.2023.110627

- Open source Multinozzle Toolpath Generator (MTG)[2]
- 6-DOF multinozzle orientation
- Toolpath error = 15 µm (6 % of D)

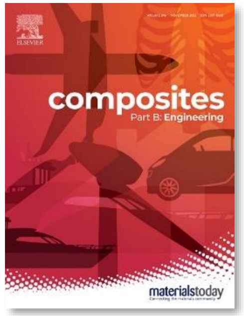

3. Study the multiprocess multinozzle additive manufacturing of an aircraft component demonstrator

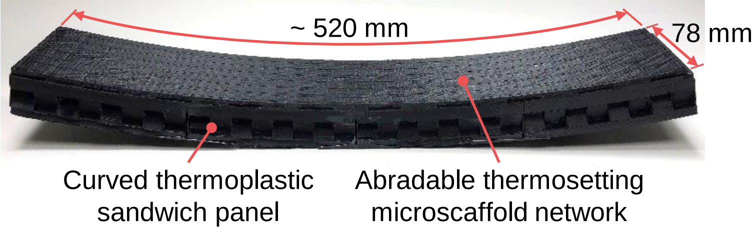

https://doi.org/10.1002/admt.202300399

- Multinozzle AM of highly viscous abradable composite
- Large-scale DIW integration into multiprocess AM
- Multilevel p max error = 4.3 %

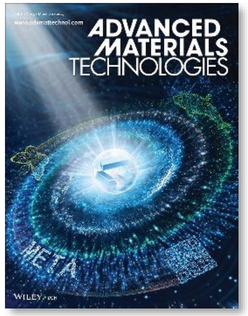

1. https://github.com/lm2-poly/mepm
2. https://github.com/lm2-poly/mtg

Industrial partners

SAFRAN
BOMBARDIER
3M
BELL
MDA
Pratt & Whitney Canada
Une société de United Technologies
VELAN

Funding

CRSNG
NSERC
Canada Foundation for Innovation
Fondation canadienne pour l'innovation
CRIAQ
Fonds de recherche
sur la nature
et les technologies
Québec
CREPEC
Centre de recherche
sur les systèmes polymères et
composites à haute performance

APPENDIX:
EXTRA SLIDES

POLYTECHNIQUE MONTRÉAL
UNIVERSITÉ D'INGÉNIERIE

LM²

ABRADABLE SEAL COATINGS

- Seal coatings to prevent air leaks
  - Allow small clearances of rotating parts

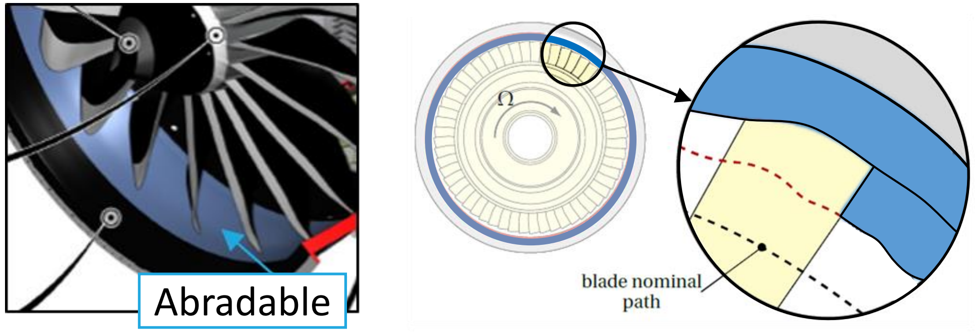

Schematic of abraded seal coating (adapted from Salvat et al., 2013)

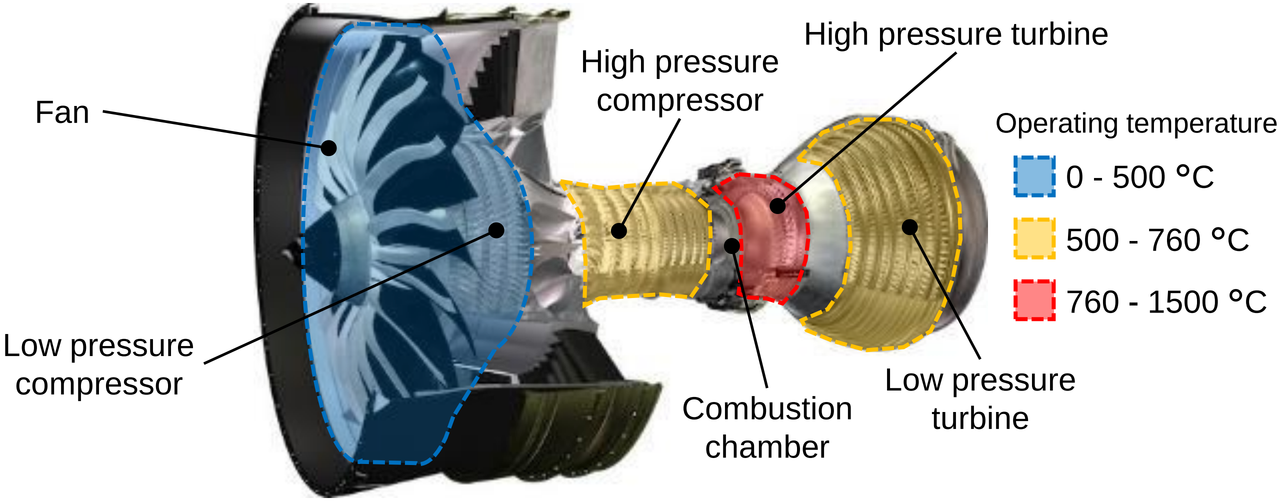

Cross section view of gas turbine engine (aerobuzz.fr)

- AM of abradable thermosetting coating
  - Microscaffolds with sound absorption potential

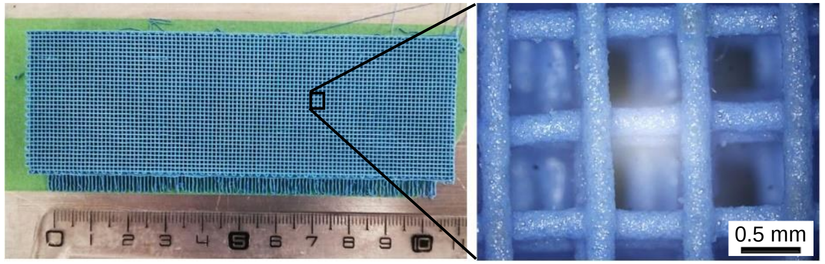

AM proof of concept of abradable microscaffold (Dubourg-Cassagne, 2015)

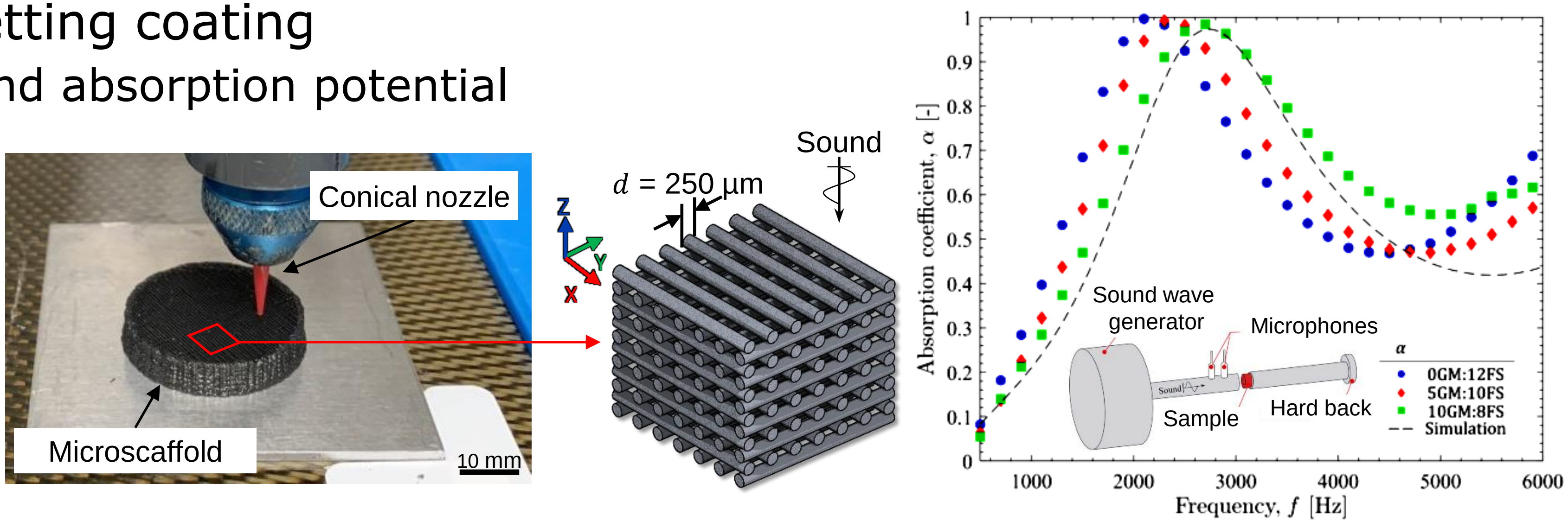

High-speed AM of abradable microscaffold for sound absorption (Brzeski et al., 2021)

SLICING FOR 3D PRINTING

- Planar slicing
  1. CAD model is tessellated in a triangle mesh
  2. Layers are "sliced" by intersecting planes with the mesh
  3. G-code is generated according to the printing parameters

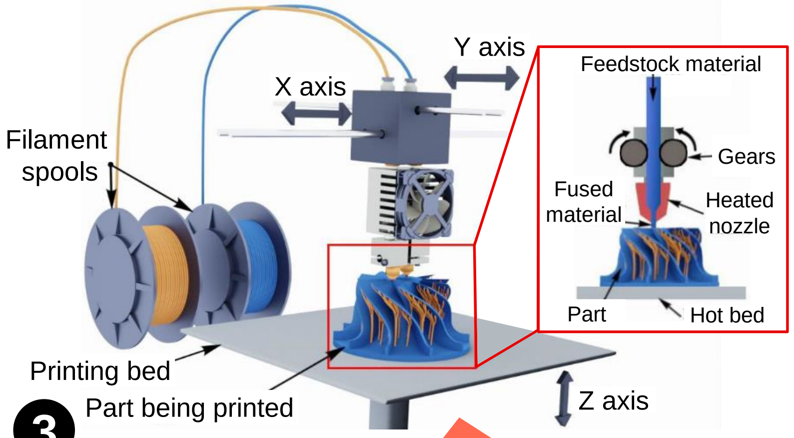

Schematic of FFF (Elkaseer et al., 2020)

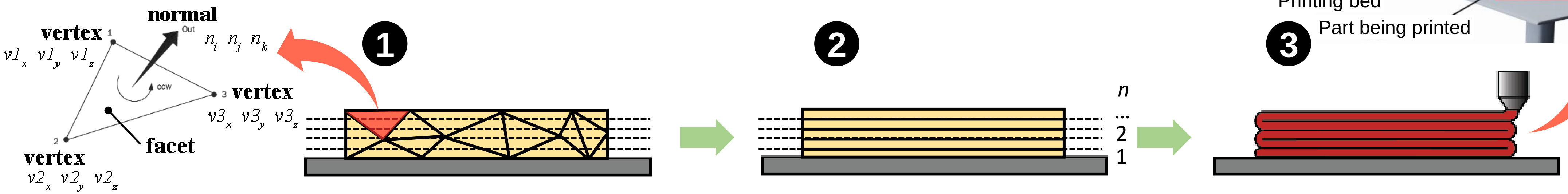

CAD model (.STL file)

Layers slicing

Layer-by-layer 3D printing

- Non-planar slicing (three selected techniques)

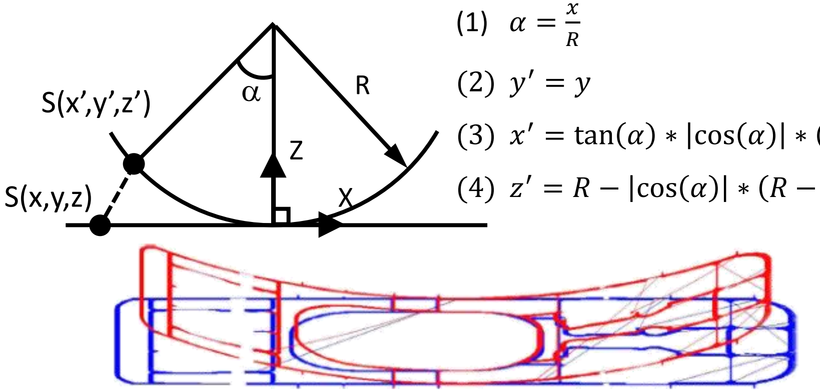

$$(1)\quad \alpha = \frac{x}{R}$$

$$(2)\quad y' = y$$

$$(3)\quad x' = \tan(\alpha) * |\cos(\alpha)| * (R - z)$$

$$(4)\quad z' = R - |\cos(\alpha)| * (R - z)$$

Cylindrical projection (Zhao et al., 2018)

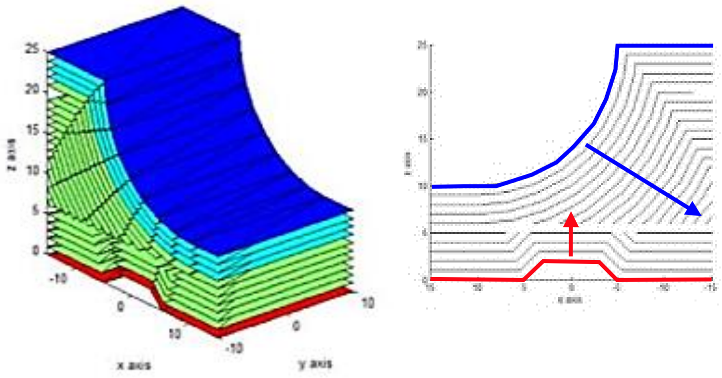

Mesh outline offset (Huang et Singamneni, 2015)

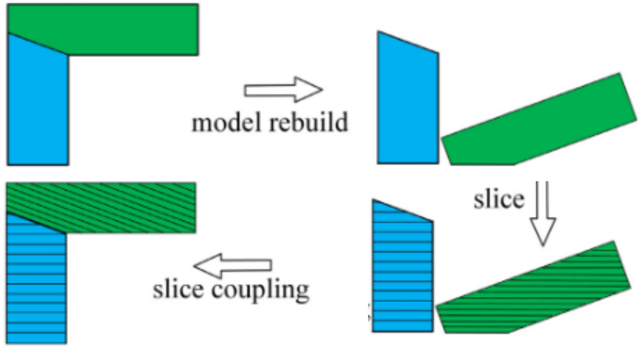

Inclined layer slicing (Zhao et al., 2018)

INDUSTRIAL 6-AXIS ROBOT ARMS

- Basic concepts and motion principles
  - Kinematic chain, joints
  - Tool Center Point (TCP)
- Potential for AM
  - Non-planar material extrusion
  - Large-scale builds

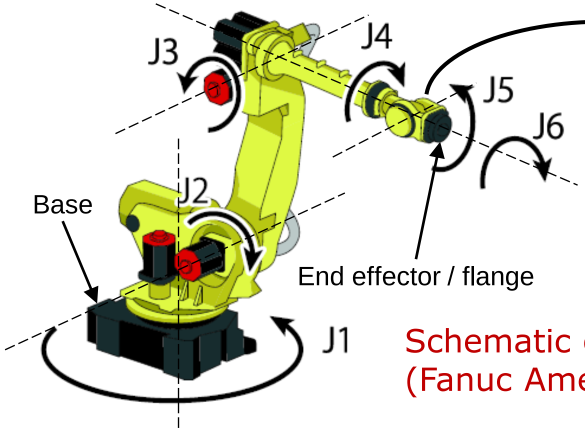

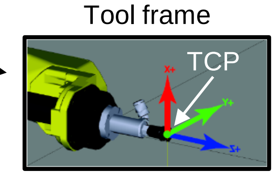

Schematic of 6-axis robot
(Fanuc America Corporation, 2018)

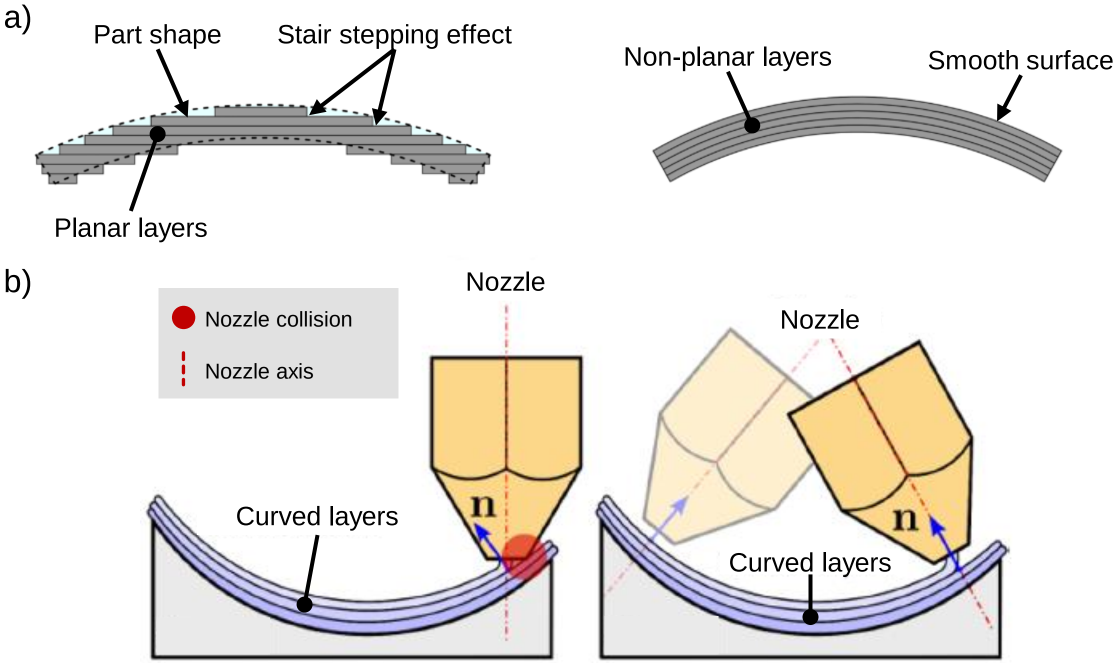

a) Schematics of non-planar slicing, b) Nozzle orientation
(adapted from Chen et al., 2019)

3D-printed bridge (Striatus project, ETH Zürich, 2021)

INDUSTRIAL 6-AXIS ROBOT ARMS

- Robotic additive manufacturing system for dynamic build orientations[1]
  - Study of gravity effect on FFF
  - Surface roughness measurement on underside of overhanging sections

a)

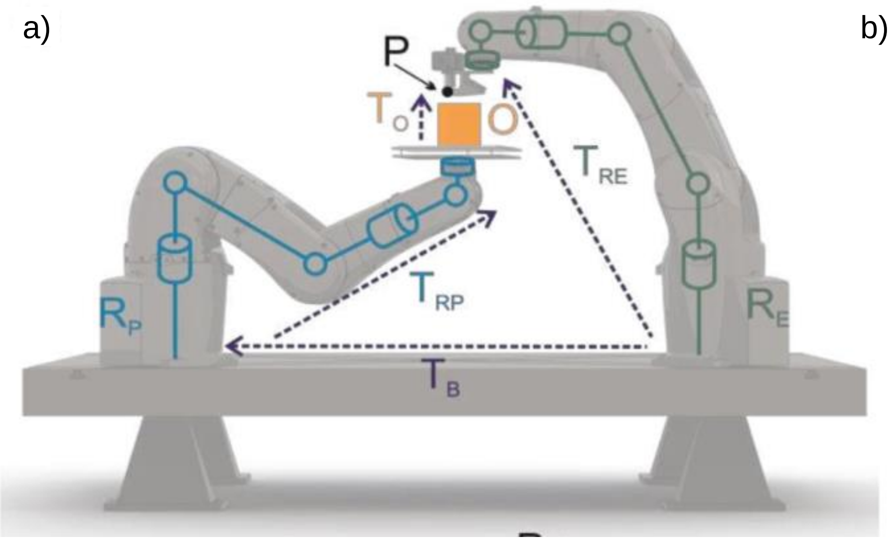

b)

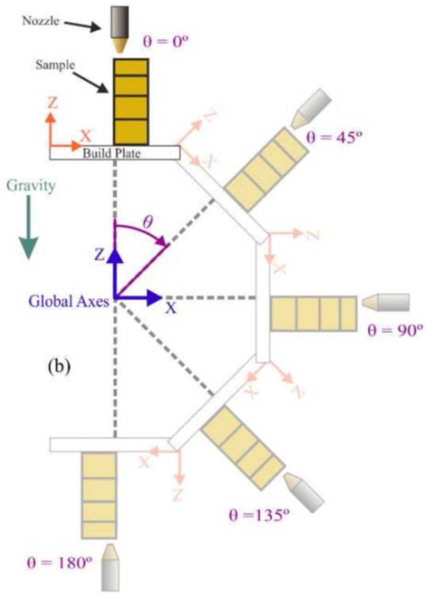

c)

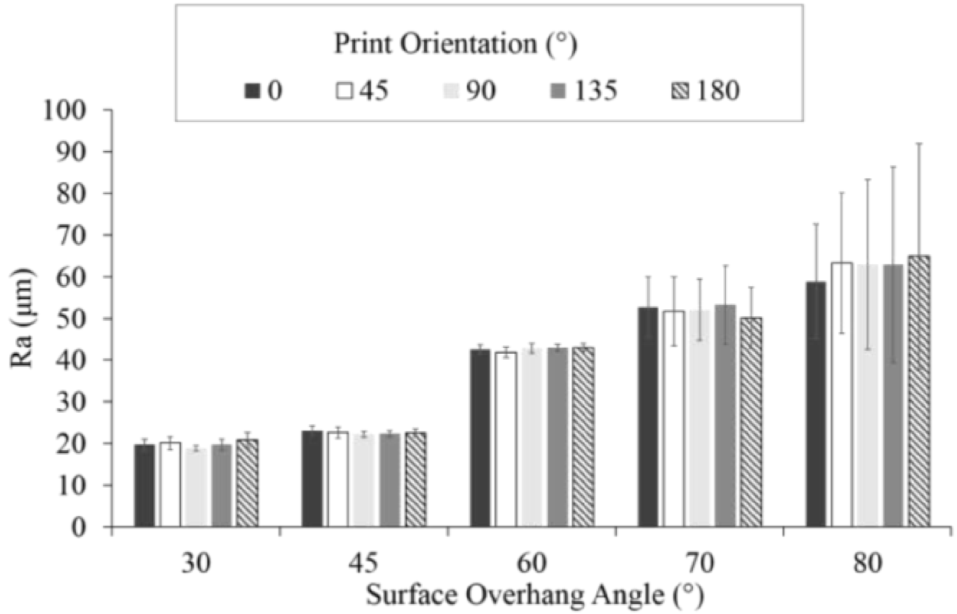

d)

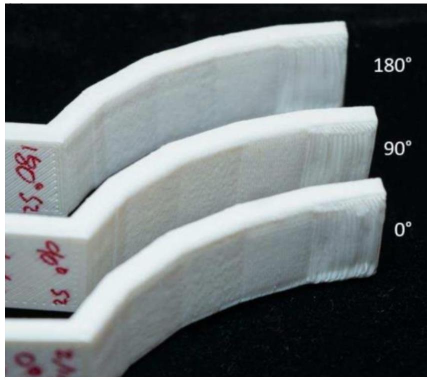

e)

Our investigation of FFF printer orientation effects is, to the best of our knowledge, the first quantitative assessment of the effect of printing at different orientations relative to gravity. Somewhat counterintuitively, we find that gravitational orientation has no impact. This is an important finding in the context of MAAM because it means that both the extruder and build tray can be rotated as necessary to maximize workspace and optimize kinematics.

1. Fry et al., Rapid Prototyping Journal, 2020

MULTINOZZLE PRINTHEADS

Authors	Highlights	Image
Khalil et al. (2005) Khalil and Sun (2007)	• 4 independent nozzles, different materials • Flow rate of 0.51 µL/s • Printing speed of 15 mm/s	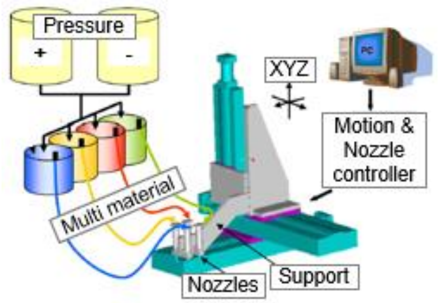
Hansen et al. (2013) Kranz (2013)	• 64 nozzles of 200 µm wide • Machined in PMMA block • Printing of 0.38 m^2 4-layer microscaffold in 25 min at printing speed of 40 mm/s	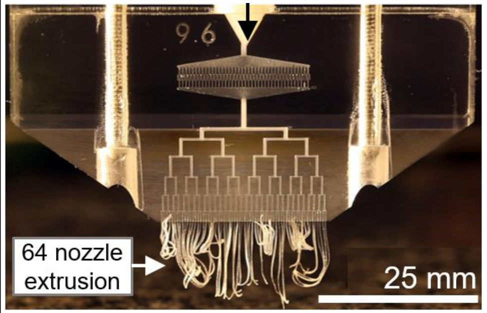
Skylar-Scott et al. (2019)	• 16 nozzles of 250 µm inner diameter • Printing speed of 40 mm/s • Multimaterial shifting frequency of 50 Hz	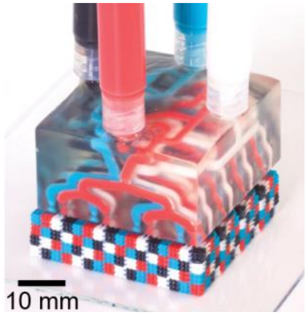

Authors	Highlights	Image
Yoon et al. (2019)	• 3 FFF extruders for **independent extrusion** (E3D volcano) • Mounted on 6-axis robot • Variable resolution (0.15 – 0.8 mm)	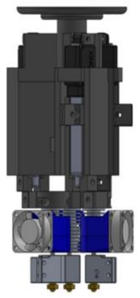
Baca and Ahmad (2020) Mhatre (2019)	• 4 FFF extruders for **simultaneous extrusion** (E3D Kraken) • Printing speed of 17 mm/s • Variable resolution (0.15 – 0.8 mm)	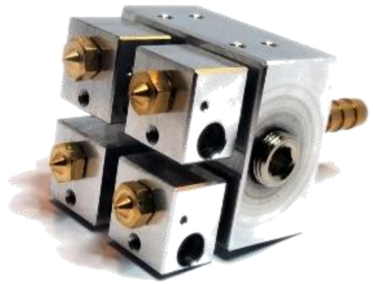
Uzel et al. (2022)	• Non-planar multinozzle AM • Variable nozzle height • Printing speed of 5 mm/s • Printing in one direction, adaptable to the substrate scanned topography	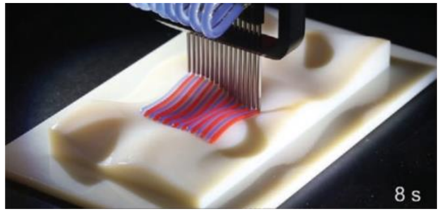

BRUNEAUX ET AL., 2008

- Characterization of process-related apparent viscosity
  - Organic ink (Therriault et al., 2005)
    - 10 → 40 wt% microcrystalline was (SP 18, Strahl & Pitsch)
    - 90 → 60 wt% petroleum jelly (Chesebrough-Pond's)
    - Non-Newtonian fluid (shear-thinning)

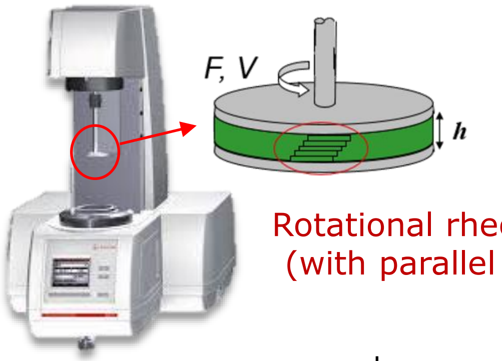

Rotational rheometer (with parallel plate)

Apparent viscosity

$$\eta_{\mathrm{app}} = \frac{\tau_W}{\dot{\gamma}_W}$$

Shear stress

$$\tau_W = \frac{P_{\mathrm{appl}} - P_a}{2(L/R)}$$

Shear rate

$$\dot{\gamma}_W = \underbrace{\frac{4Q}{\pi R^3}}_{\dot{\gamma}_{\mathrm{Newt}}}\left(\frac{3+b}{4}\right)$$

Rabinowitsch correction

$$b = \frac{d\log(\dot{\gamma}_{\mathrm{Newt}})}{d\log(\tau_W)}$$

Power-law model for viscosity[1] (GNF)

$$\eta(\dot{\gamma}) = m\dot{\gamma}^{n-1}$$

Hagen–Poiseuille law[1]

$$Q = \frac{\pi(\mathcal{P}_0 - \mathcal{P}_L)R^4}{8\mu L}$$

Carreau–Yasuda model[1]

$$\frac{\eta(\dot{\gamma}) - \eta_\infty}{\eta_0 - \eta_\infty} = \left[1 + (\dot{\gamma}\lambda)^a\right]^{\frac{n-1}{a}}$$

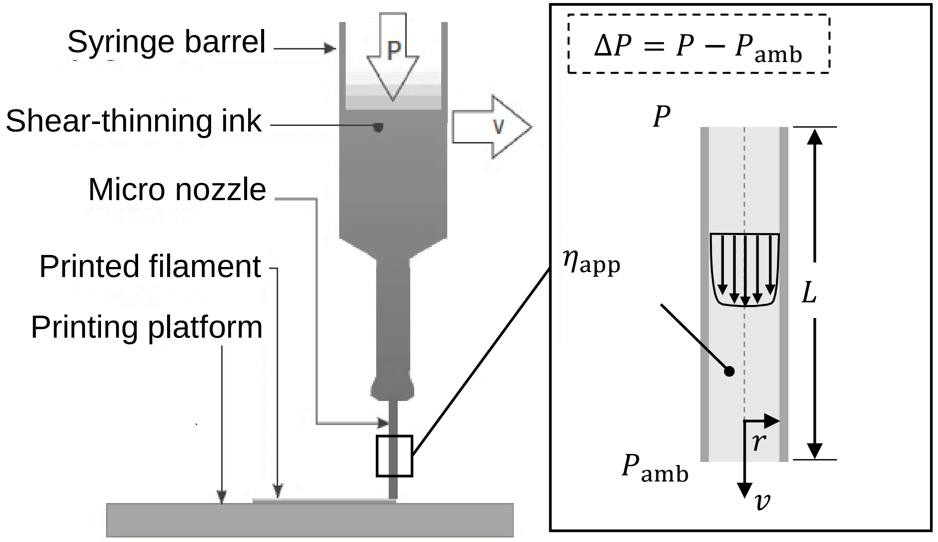

Characterization of process-related apparent viscosity (Bruneaux et al., 2008)

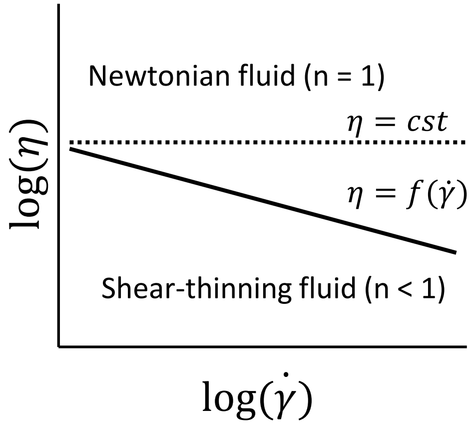

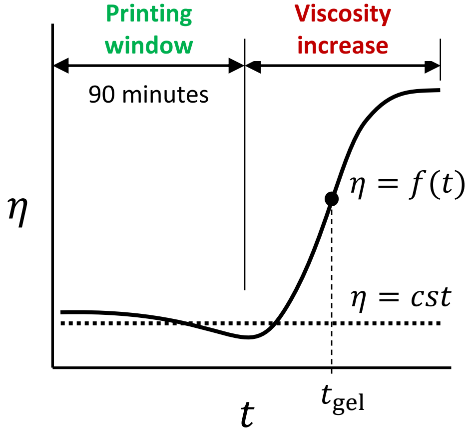

1. Morrison, *Understanding rheology*, Oxford University Press, 2021.

MEPM EQUATIONS

- Pressure gradient calculation

Apparent viscosity (η_{app})

(1) $Q_i = v\, A_{nozzle}$

(2) $\dot{\gamma}_i = \frac{32\, Q_i}{\pi\, D^3}\left(\frac{3+1/n}{4}\right)$

(3) $\eta_{app,i} = K\, \dot{\gamma}_i^{\,n-1}$

K: Consistency index (Pa.s^n)
n: Power-law index (-)
($n < 1$ for shear-thinning fluid)

Pressure gradient (ΔP)

(4) $R_i = \frac{128\, L\, \eta_{app,i}}{\pi\, D^4}\left(\frac{3+1/n}{4}\right)$

(5) $R_{eq} = \frac{1}{\sum_{i=1}^{\alpha} \frac{1}{R_i}}$ (for nozzles in parallel)

(6) $\Delta P = R_{eq} \sum_{i=1}^{\alpha} Q_i$

α: Number of nozzles

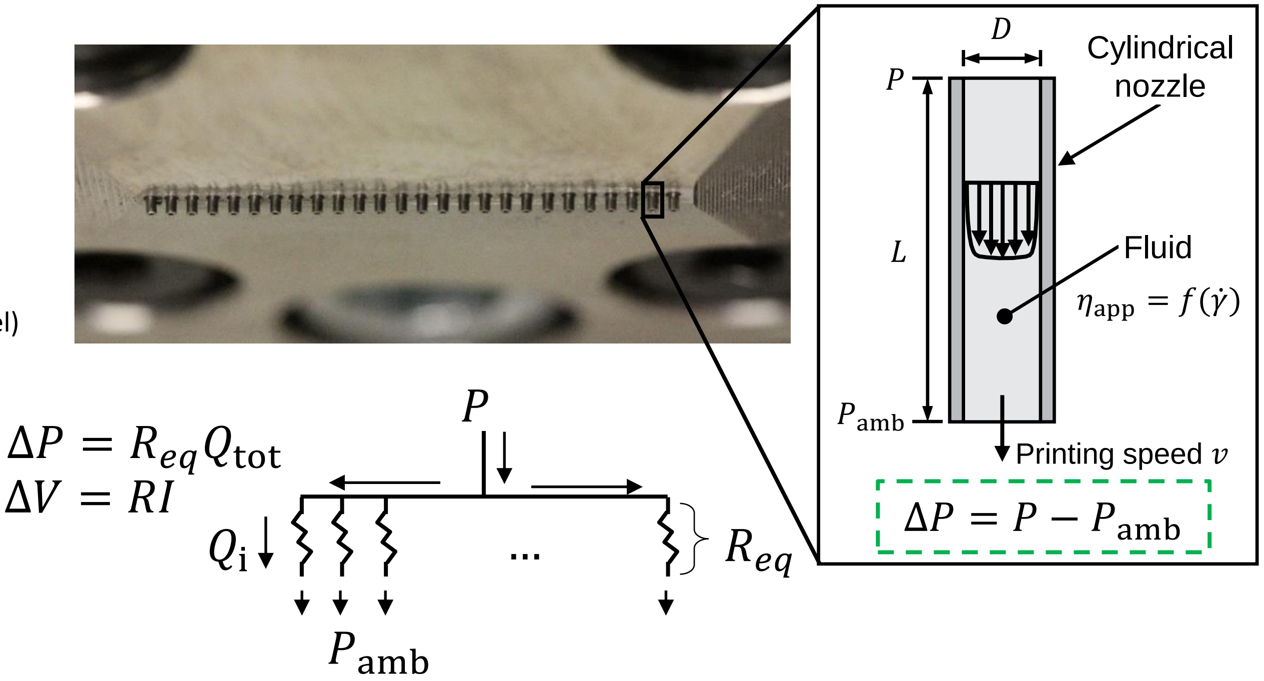

- Total volumetric flow rate calculation

(7) $Q_{i,guess} = Q_i$ ← Find new R_i with imperfect nozzles

(8) $Q_{i,new} = \frac{\Delta P}{R_i}$

(9) $\Delta Q_i = \frac{|Q_{i,new} - Q_{i,guess}|}{Q_{i,guess}} < 10^{-4}$? → No → (10) $Q_{i,guess} = Q_{i,new}$

Yes ↓

(11) $Q_{tot} = \sum_{i=1}^{\alpha} Q_{i,new}$

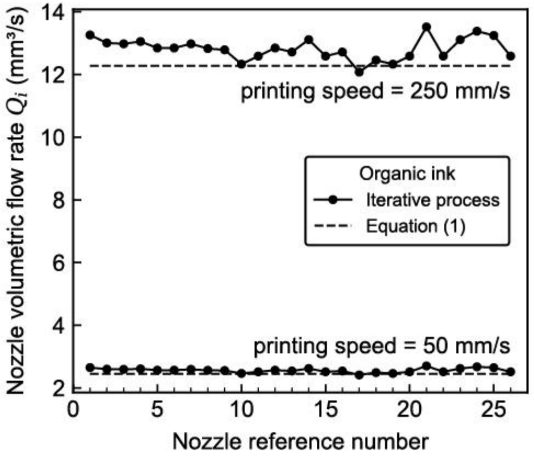

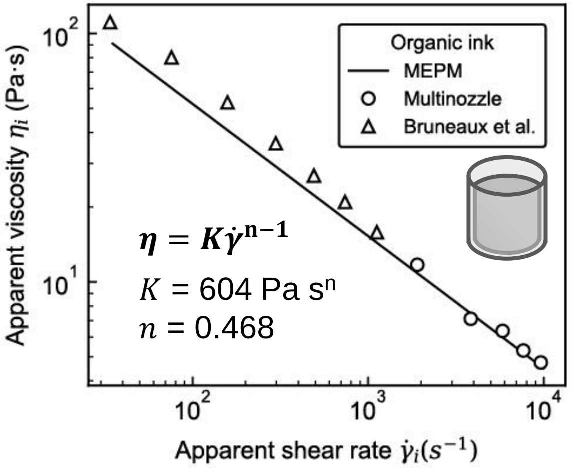

MEPM EQUATIONS

- Flow resistance equation
  - Hagen-Poiseuille flow rate of Newtonian fluid in pressure-driven flow in a pipe :

(1) $v(r) = \frac{(P_0 - P_L)(R^2 - r^2)}{4\eta L}$

(2) $Q = v_{eff}\, A$

(3) $Q = \frac{(P_0 - P_L)R^2}{4\eta L} \cdot \frac{\pi R^2}{2}$

(4) $Q = \frac{\pi (P_0 - P_L) R^4}{8\eta L}$

(5) $\frac{Q 8\eta L}{\pi R^4} = (P_0 - P_L)$

(6) $\Delta P = \frac{128\eta L}{\pi D^4} Q = RQ$

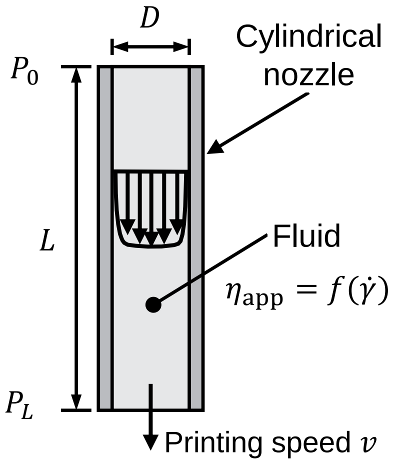

$$\boxed{\Delta P = P_0 - P_L}$$

  - Can also be obtained using the definition of viscosity :

(1) $\eta = \frac{\tau}{\dot{\gamma}}$

(2) $\eta = \frac{\frac{\Delta P}{2L/R}}{\frac{4Q}{\pi R^3}}$

(3) $\eta = \frac{\Delta P \pi R^3}{2\frac{L}{R} 4Q}$

(4) $\eta = \frac{\pi R^4}{8LQ} \Delta P$

(5) $\Delta P = \frac{8LQ}{\pi R^4} \eta$

(6) $\Delta P = \frac{8\eta L}{\pi R^4} Q = \frac{128\eta L}{\pi D^4} Q$

(7) $\Delta P = \left(\frac{3 + 1/n}{4}\right) \frac{128\eta L}{\pi D^4} Q$

  - For non-Newtonian fluid, we must add the Rabinowitsch correction :

(7) $\Delta P = \left(\frac{3 + 1/n}{4}\right) \frac{128\eta L}{\pi D^4} Q$

(8) $R = \left(\frac{3 + 1/n}{4}\right) \frac{128\eta L}{\pi D^4}$

MEPM EQUATIONS

- Matlab program for multinozzle extrusion prediction 
    - Input = printing speed (v), material viscosity parameters (K, n), nozzle geometry (D, L, α)
    - Output = required pressure (ΔP), total volumetric flow rate (Q_{tot})
    - Organic ink

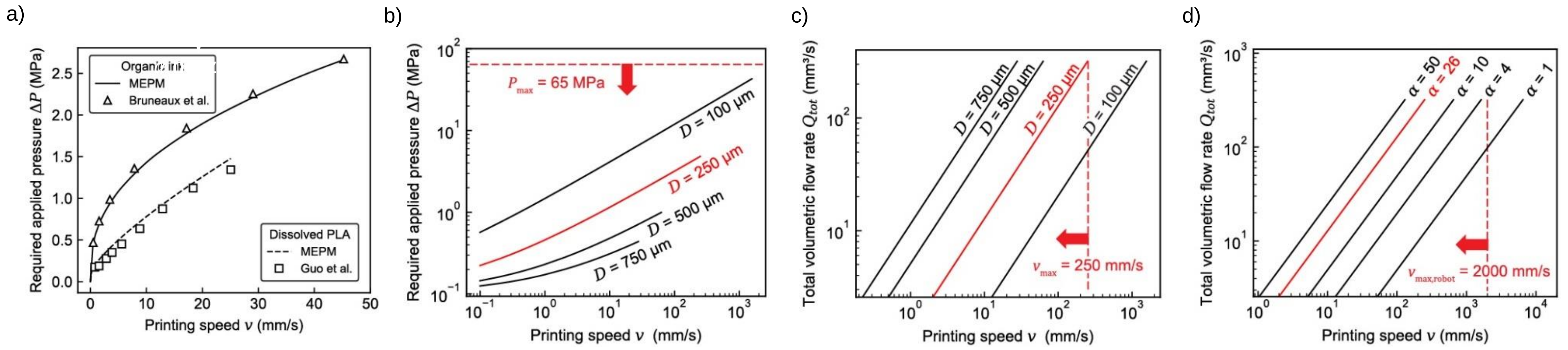

a) Validation with organic ink[1] and dissolved PLA[2] (single nozzle), b), c), d) Exploration of multinozzle configurations

1. Bruneau et al., J. Micromechanics Microengineering, 2008
2. Guo et al., Langmuir, 2014

MEPM EQUATIONS

- Simulation of clogged nozzles
  - Organic ink, v = 50 mm/s
  - Nozzle diameter = 0 mm
  - Reservoir piston speed is unchanged

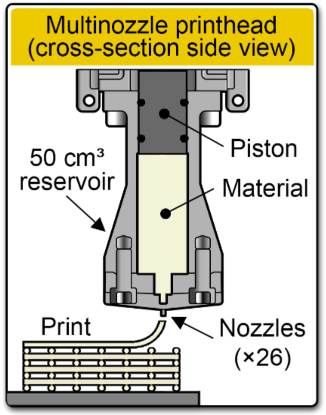

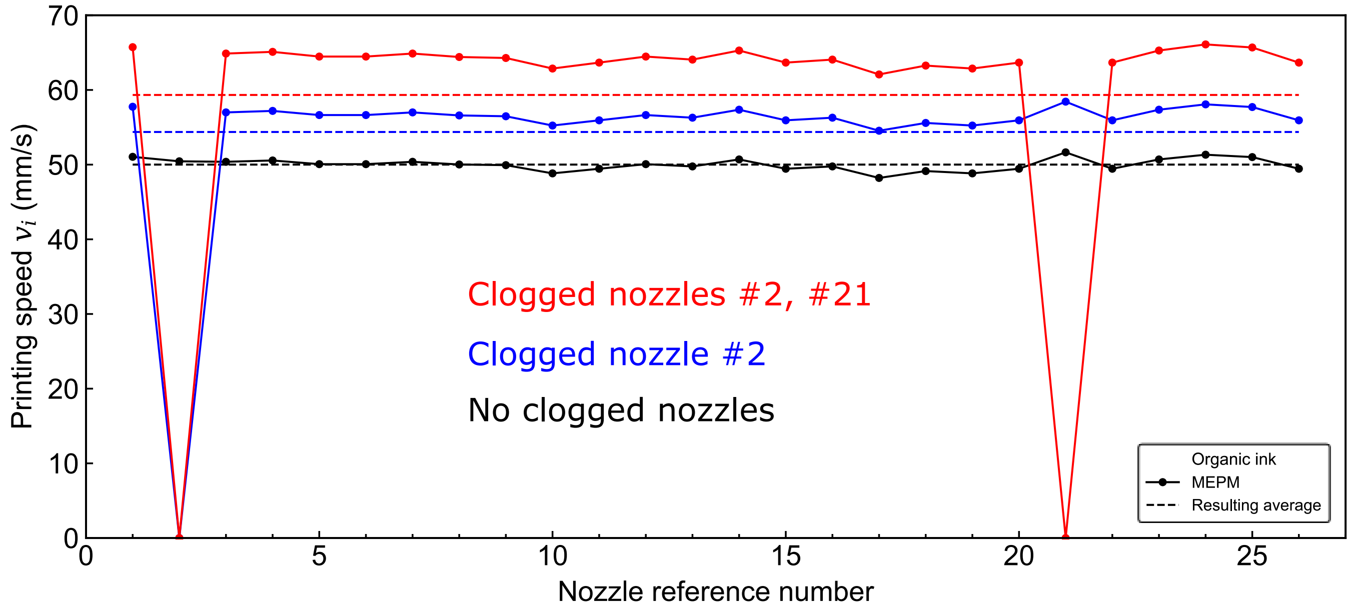

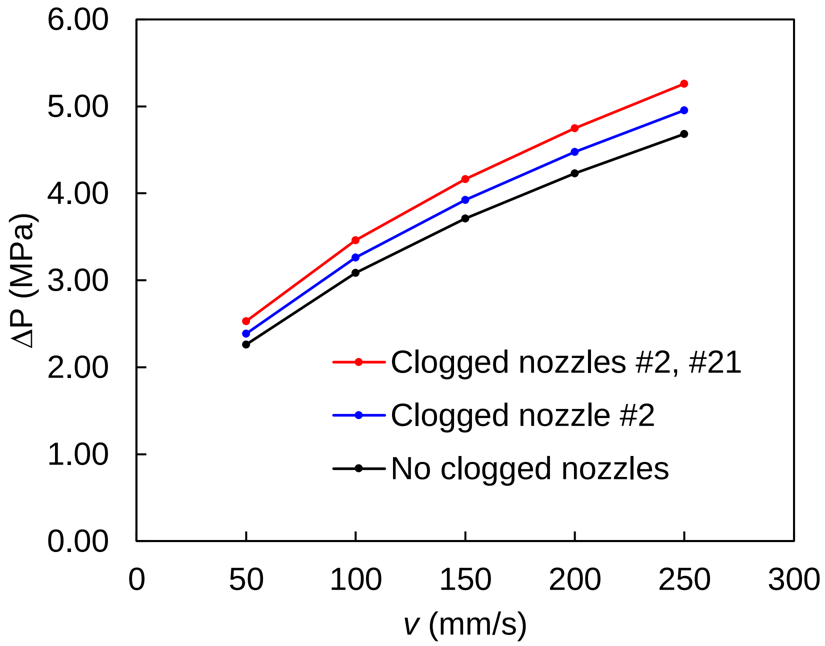

Simulation of clogged nozzles using the MEPM. Clogged nozzles are simulated by setting their diameter to zero.

MICROSCAFFOLD NETWORK TYPICAL GEOMETRY

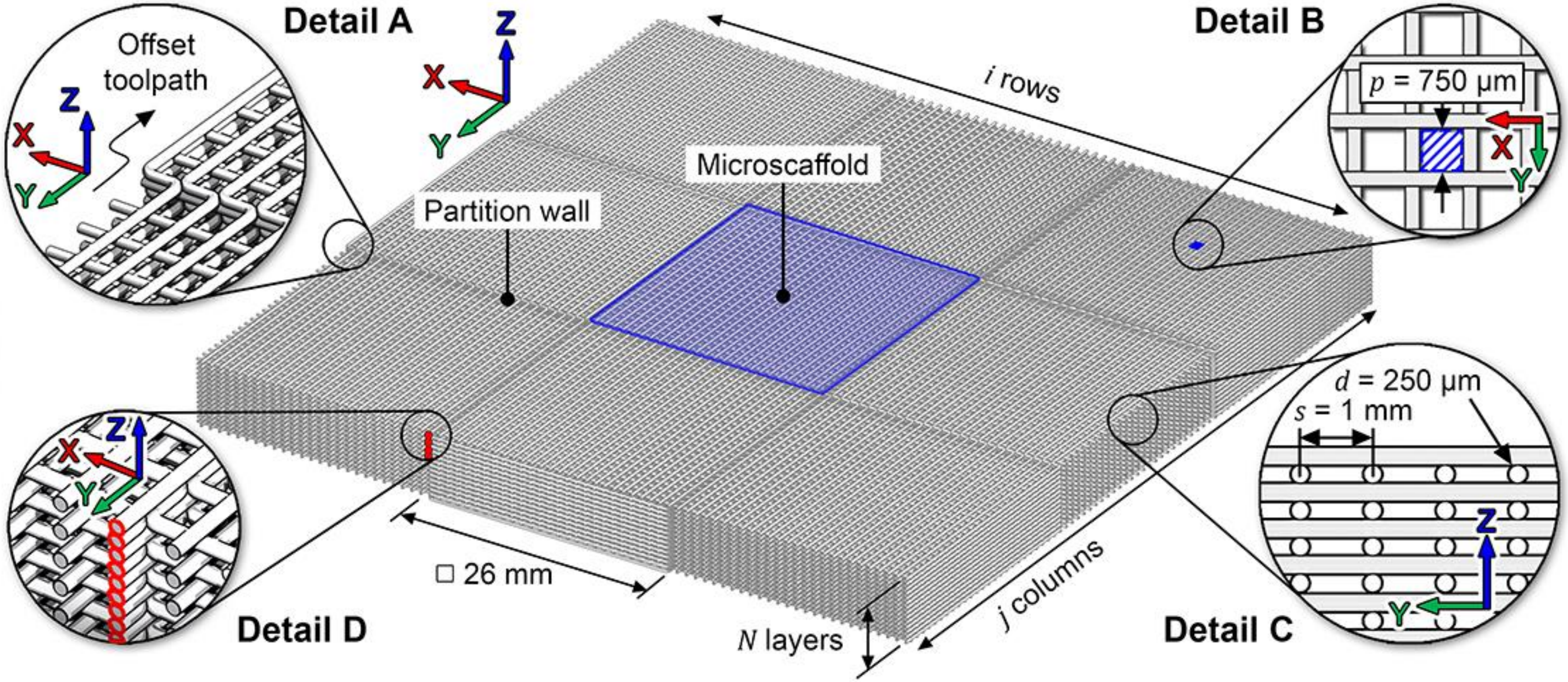

OTHER PLANAR PRINTING CASE STUDIES

- Large partitioned microscaffold network

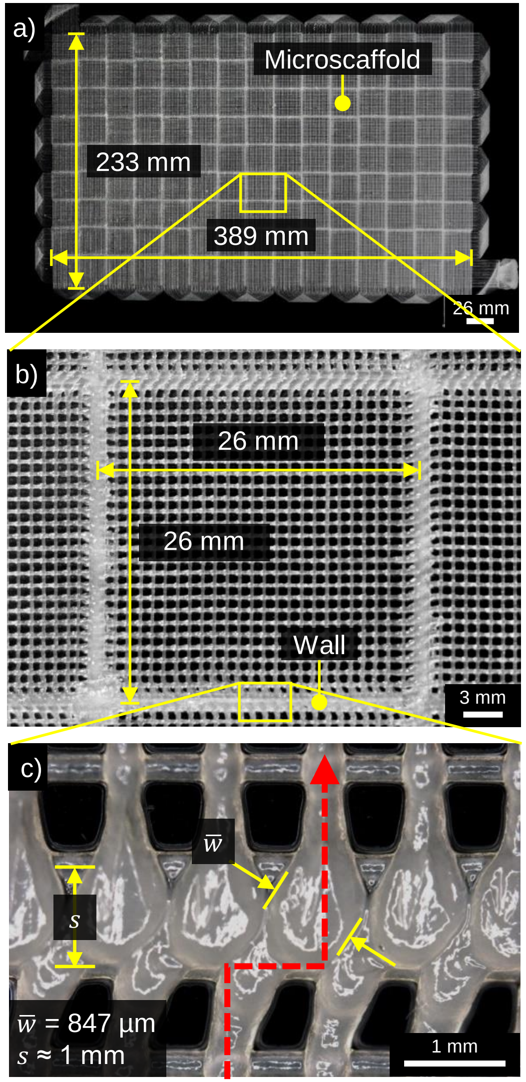

Programmed toolpath

- 9 × 15 network
- ΔP = 2.40 MPa
- $\boldsymbol{v}$ **= 50 mm/s**
- Q_{tot} = 63.2 mm³/s
- 8 min 45 s

- **9 × 10⁴ mm²**
- 5 layers
- Wall features

- Slow-down
- **Desynchronization** of **motion** and **extraction**
- Over-extrusion

- Variable pore size microscaffold network

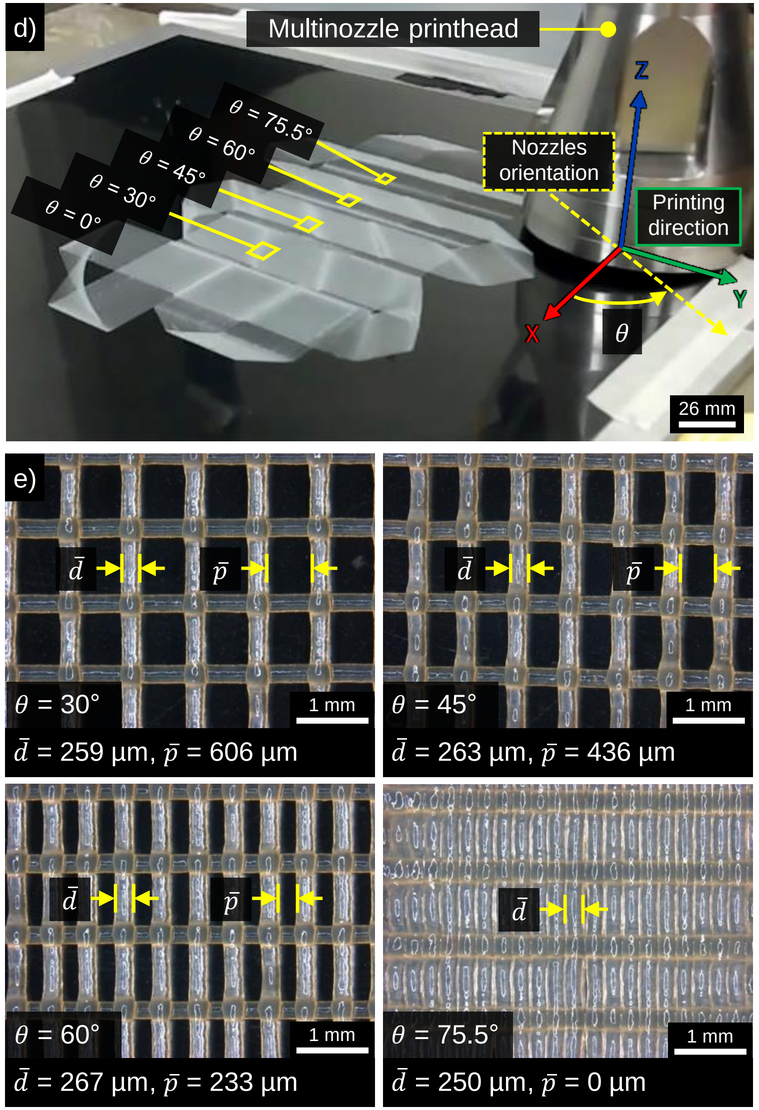

- 3 × 5 network
- v = 50 mm/s

- 2 layers
- $\boldsymbol{\theta}$ **increase**

$$p_{\text{theo}} = s \cdot cos\theta - d$$

$\boldsymbol{\theta}$	p_{theo} (µm)	$\bar{p}$ (µm)	Error (%)
0	750	736	2
30	616	606	2
45	457	436	5
60	250	233	7
75.5	0	0	-

MTG VISUALIZATION FOR SINUSOIDAL SURFACE

- MTG V5.6, 2023
- Single curvature sinusoidal surface
  - Max Δz = 2.2D (limit Δz = 24.2D)
  - Uneven spacing due to toolpath distortion

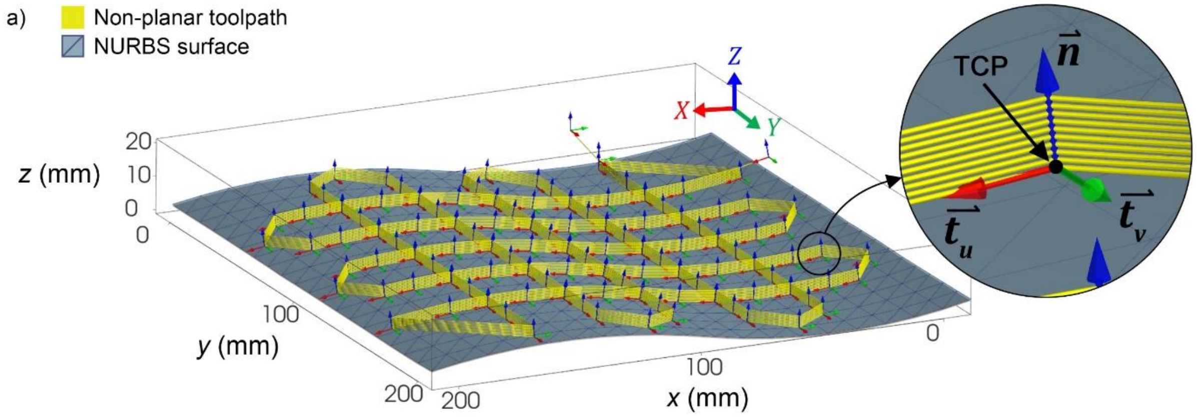

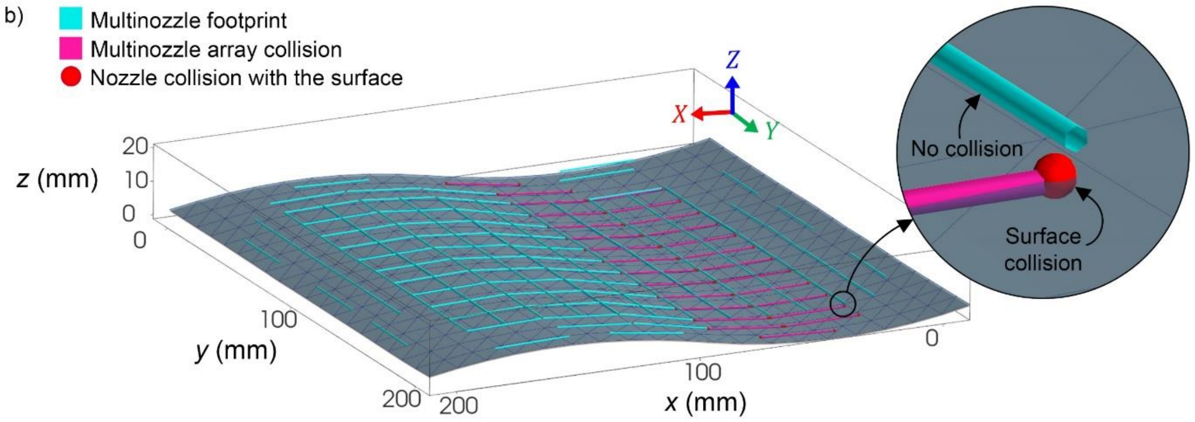

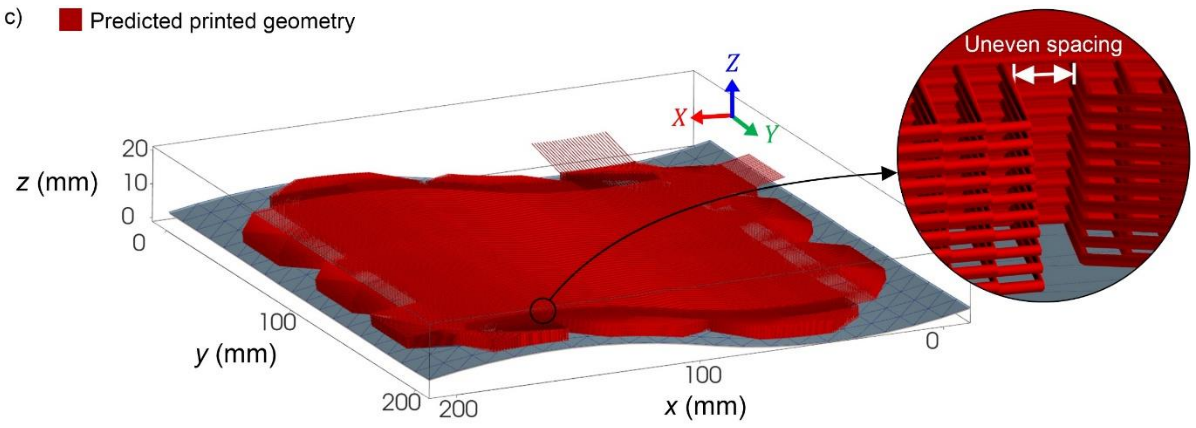

EFFECT OF RELATIVE DISTANCE BETWEEN NOZZLE TIPS AND SUBSTRATE TOP SURFACE

- Limit $\Delta z = 24.2D$
  - https://www.youtube.com/watch?v=VeQNQTJUrB4
  - https://www.youtube.com/watch?v=Sd902JQLBzU

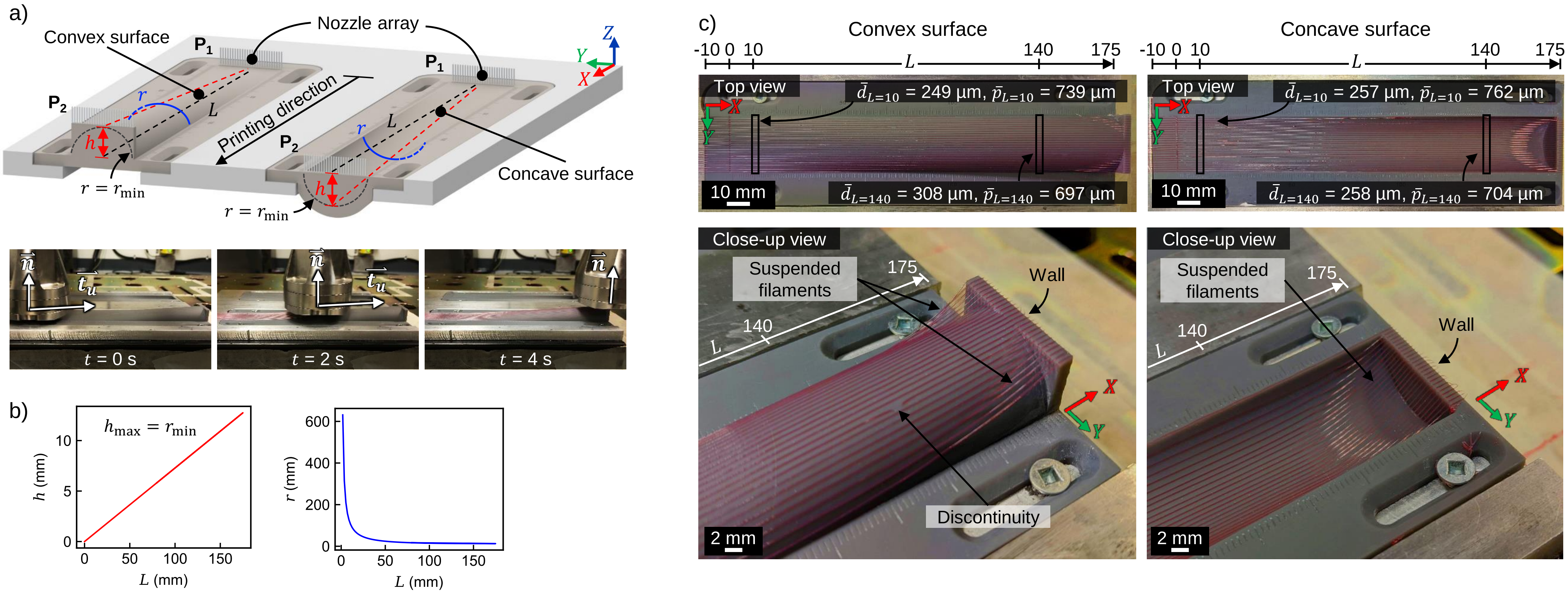

$$\Delta z = h + D$$

NON-PLANAR SUBSTRATE

- Substrate topography acquisition
  - Challenge : experimental reference frame calibration
  - Sinusoidal surface : validation of the non-planar AM method

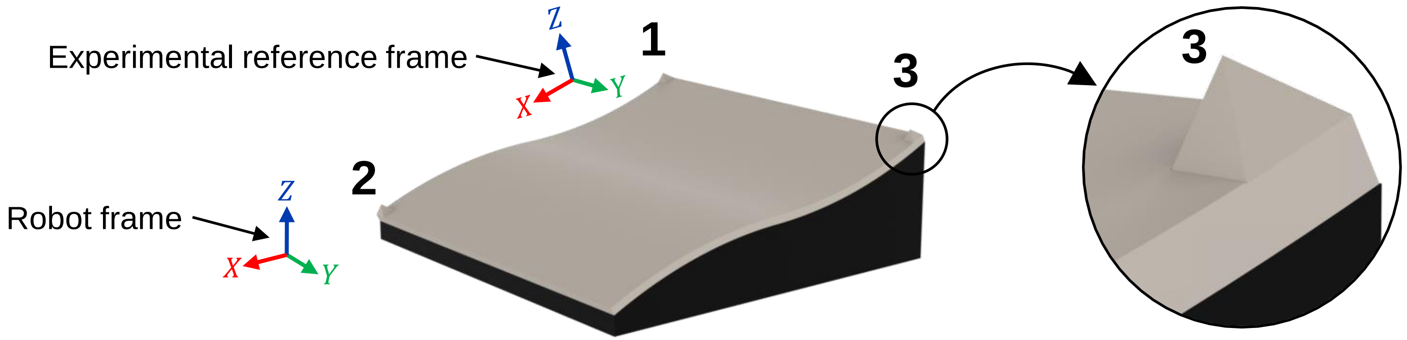

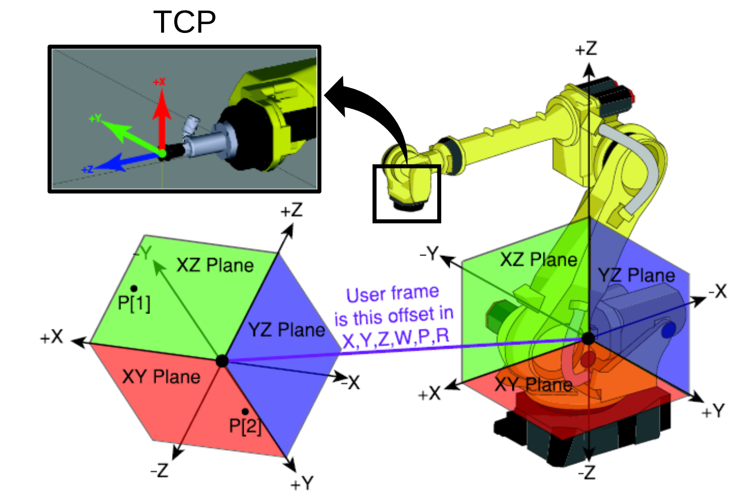

Experimental reference frame   Robot frame

Step 1 : Non-planar surface scan

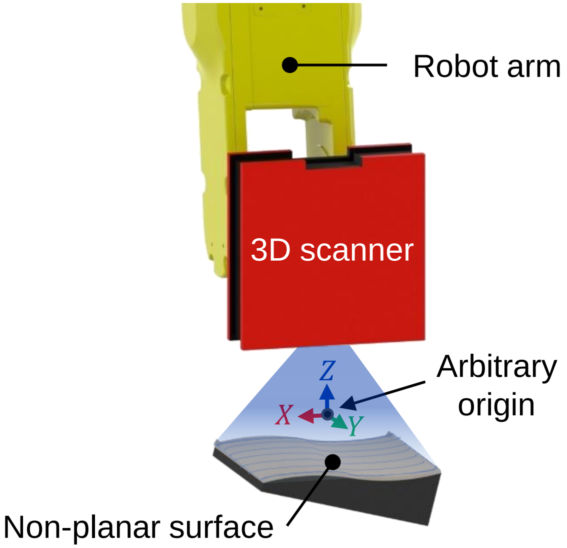

Step 2 : Mesh reference frame creation

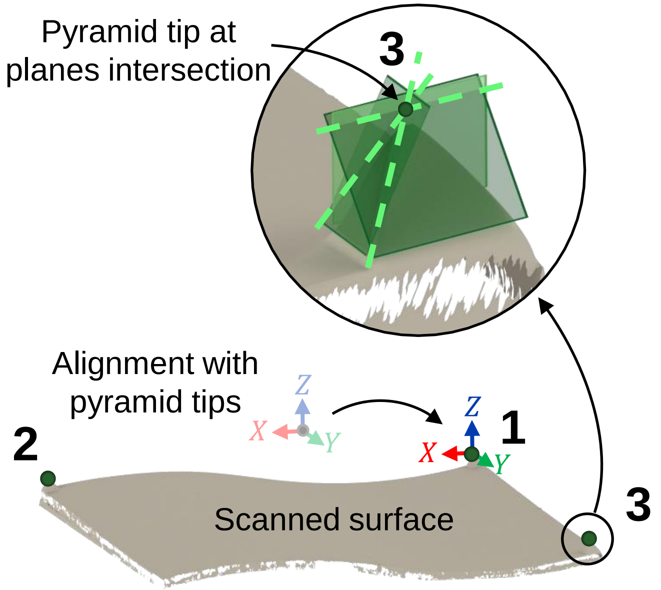

Step 3 : Experimental reference frame creation

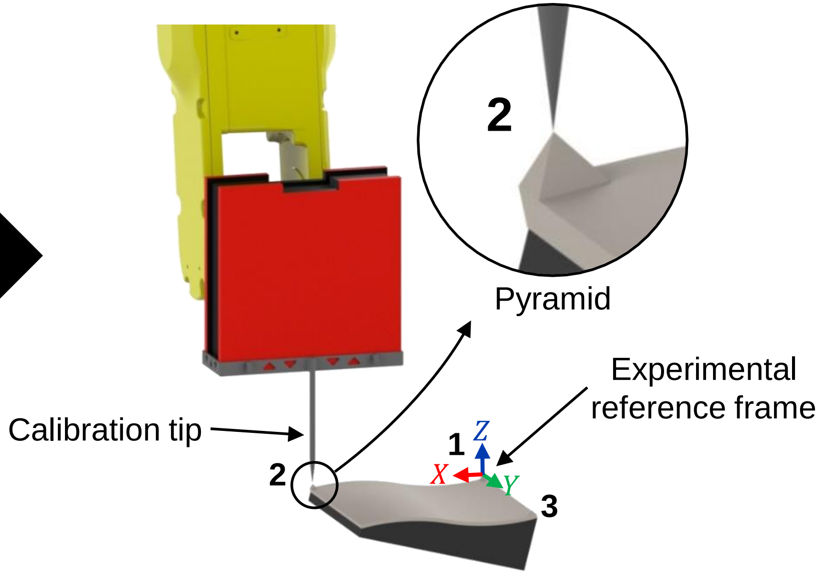

NON-PLANAR MICROSCAFFOLD NETWORKS

- Single curvature sinusoidal surface

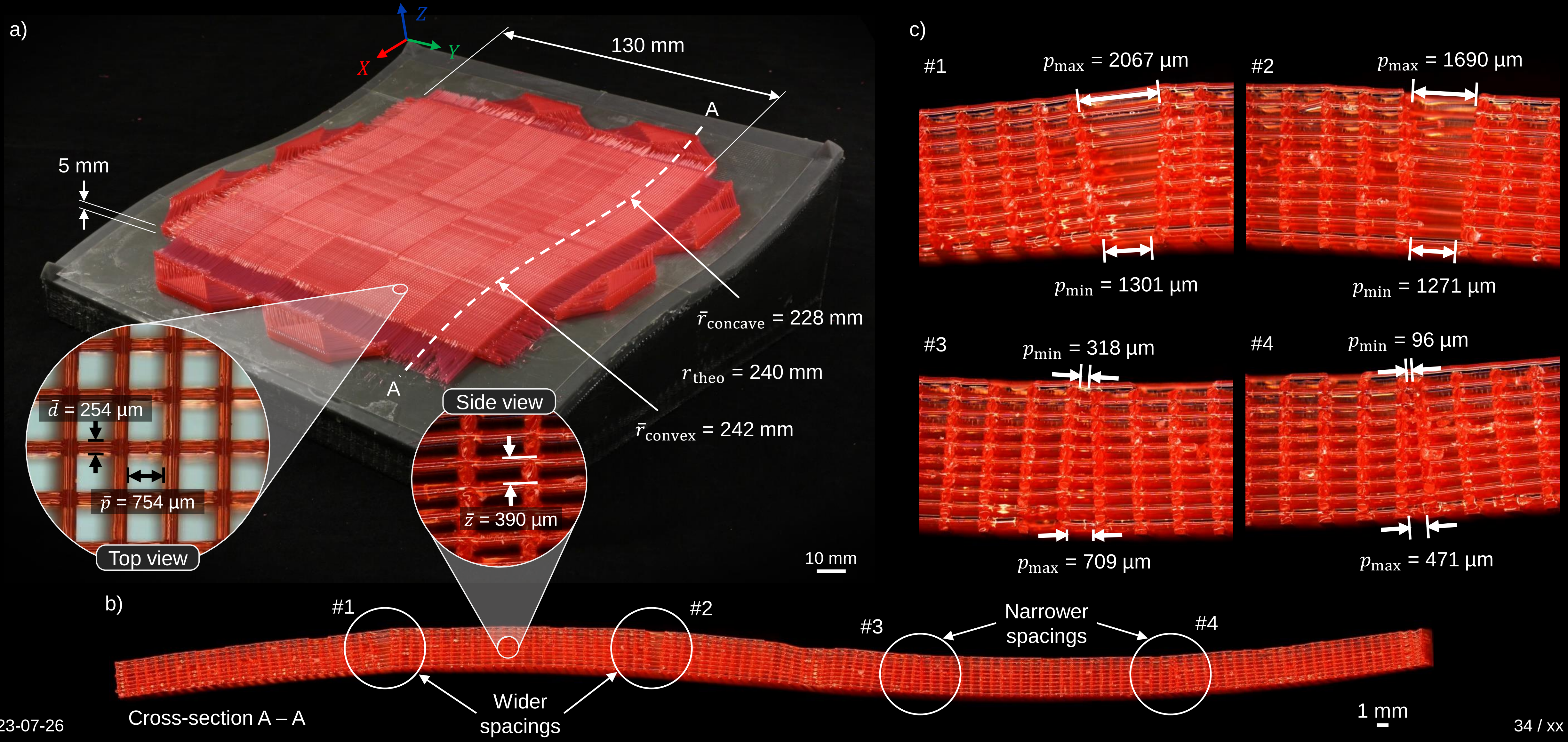

ABRADABLE MATERIALS FOR AM

- Abradable material formulations development process map[1]
  - Using hydrophilic fumed silica (Evonik Aerosil 200)

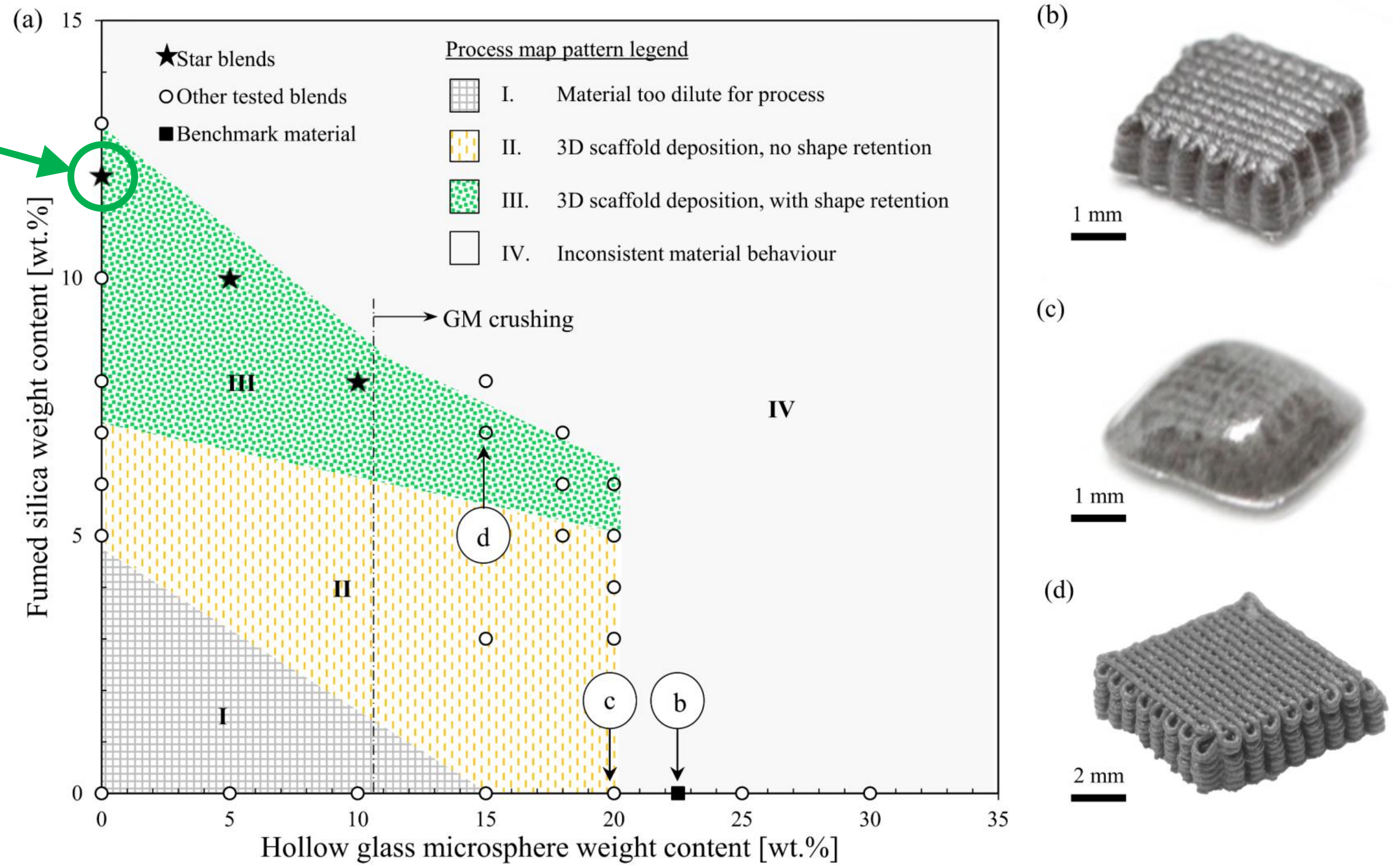

1. Brzeski et al., Additive Manufacturing, 2021

MATERIALS COMPARISON

- Summary of materials used in this research project

Material	Composition	Density (g/cm³)	Power law parameters
Organic ink	60 wt% petroleum jelly 40 wt% microcrystalline wax	0.905	K = 604 Pa s^n n = 0.468
Epon formulation	10 wt. part Epon 828 resin 4 wt. part Epikure 3274 curing agent 14 wt.% hydrophilic fumed silica	1.214	K = 10,120 Pa s^n n = 0.2429
Abradable formulation[1]	94 wt. part EC-3524 Part A (neat curing agent) 100 wt. part EC-3524 Part B (neat resin) 12 wt.% hydrophobic fumed silica	1.279	K = 6,673 Pa s^n n = 0.3578

a)

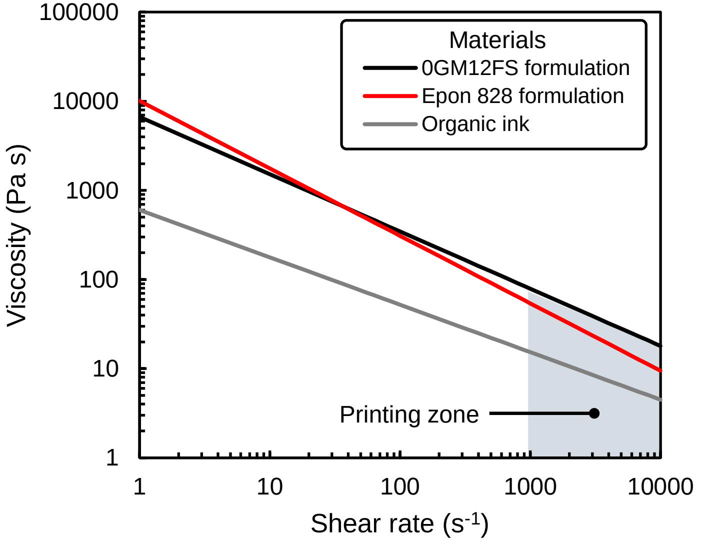

b)

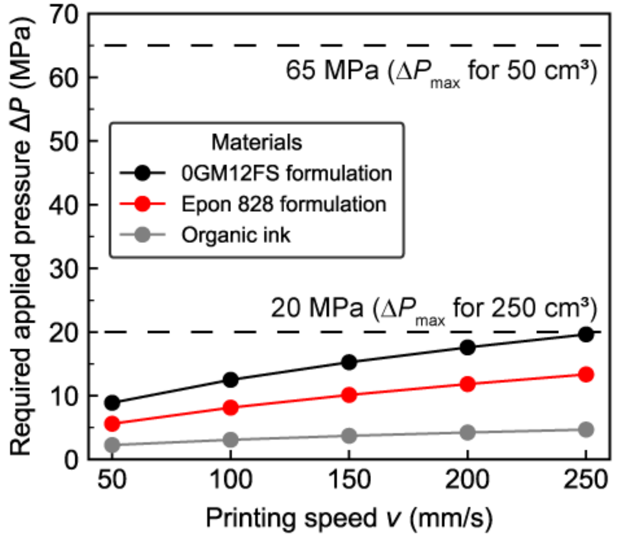

c)

ΔP_{max} = 65 MPa ΔP_{max} = 20 MPa

1. In collaboration with Dr. Iee Lee Hia and M. David Brzeski

NON-PLANAR MULTINOZZLE AM CONSIDERATIONS

- Collision avoidance (TCP offset from surface)

Avoid nozzles collision with the curved surface (offset h)

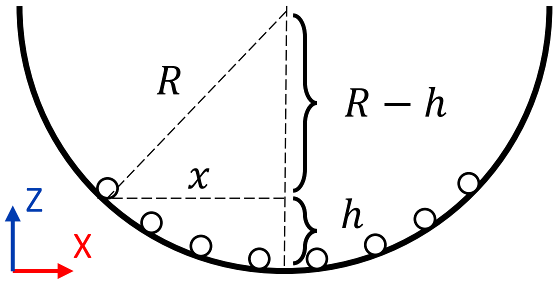

$$h = R - \sqrt{R^2 - x^2}$$

$\boldsymbol{R}$: surface radius
$\boldsymbol{x}$: multinozzle ½ width
$\boldsymbol{h}$: tool offset to avoid collision
○ : filament (d = 250 µm)

For example:
Curved surface
R = 1 m
h = 78 µm

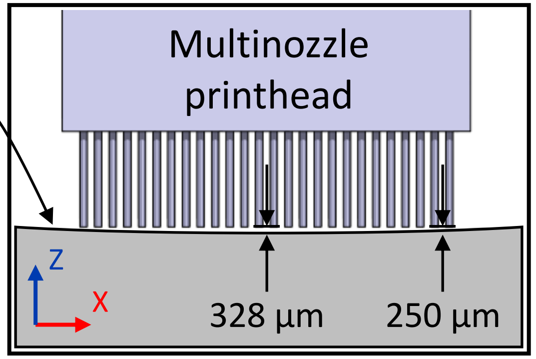

- Pore size adjustment across the layers

Adjust inter-filament distance p for each layer

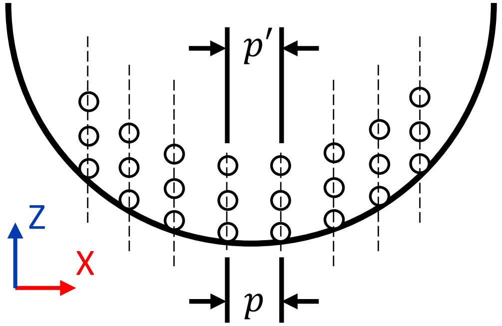

Non-adjusted distance $p = p'$

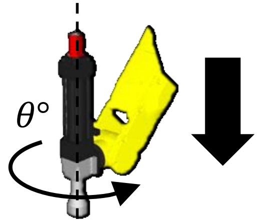

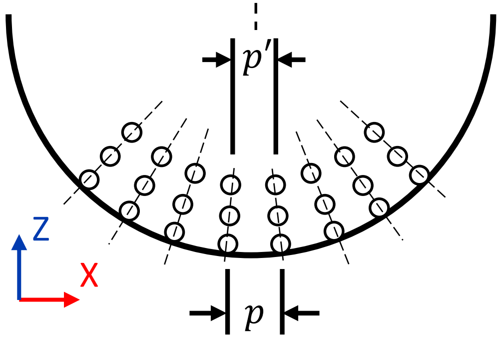

Adjusted distance $p > p'$

PORE SIZE ADJUSTMENT

- Pore size variation across the layers using variable θ

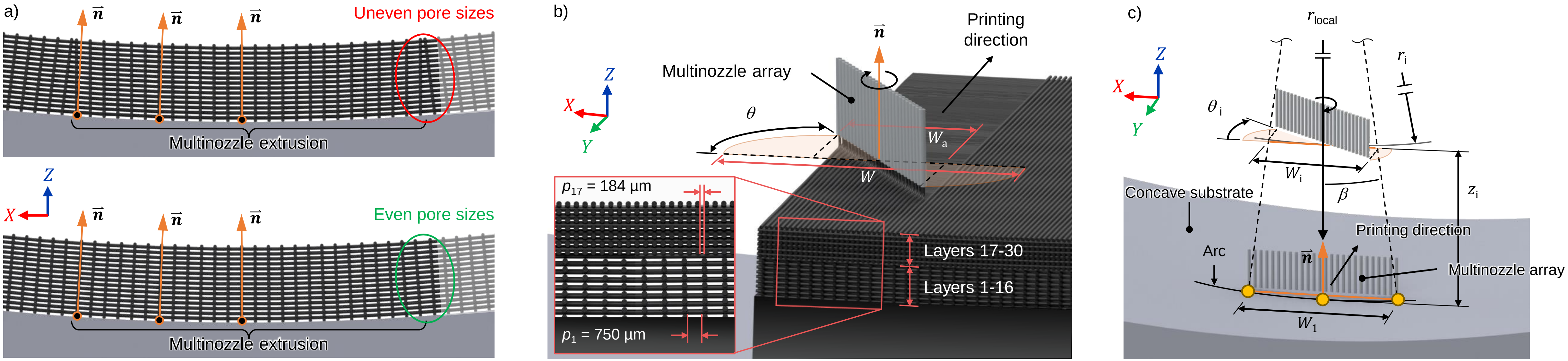

- θ calculation as function of local radius

(1) $\beta = \tan^{-1}\left(\frac{W_1}{2 \cdot r_{local}}\right)$

(2) $r_i = r_{local} \pm z_i$

(3) $W_i = 2 \cdot r_i \cdot \tan(\beta)$

(4) $\delta\theta_i = \cos^{-1}\left(\frac{W_i}{W}\right) - \theta_{i-1}$

(5) $\theta_i = \theta_{i-1} + \delta\theta_i$

- Pore size p calculation

(6) $p_i = s\ cos\theta - d$

(7) $p_i = (p + d)\left(\frac{r_{local} \pm z_i}{r_{local}}\right) - d$

ERROR p RESULTING FROM ASSEMBLY ERROR

- Assembly error sources
  - Two interfaces assembled with screws
  - No locating pins
  - Unknown θ error

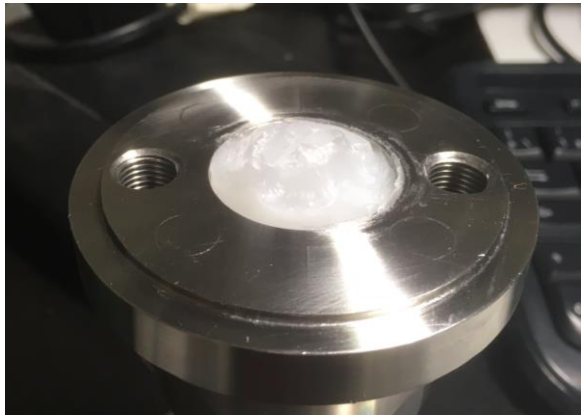

Reservoir assembly (×2 screws)

Printhead assembly (×4 screws)

Target *p* = 750 µm				
Target θ (°)	**θ (°)**	***p* (mm)**	**Error *p* (mm)**	**Error *p* (%)**
0	0	0.750		
Error θ (°)				
+ 7.1	7.1	0.742	0.008	1.02%
- 7.1	-7.1	0.742	0.008	1.02%
+ 2.0	2.0	0.749	0.001	0.08%
- 2.0	-2.0	0.749	0.001	0.08%

Target *p* = 184 µm				
Target θ (°)	**θ (°)**	***p* (mm)**	**Error *p* (mm)**	**Error *p* (%)**
64.28	64.28	0.184		
Error θ (°)				
+ 0.5	64.78	0.176	0.008	4.28%
- 0.5	63.78	0.192	-0.008	-4.26%
+ 2.0	66.28	0.152	0.032	17.23%
- 2.0	62.28	0.215	-0.031	-16.95%

LIGHTWEIGHT POTENTIAL

- Aircraft component as a lightweight part : density comparison
  - Benchmark : helium gas pycnometer[1]
  - Microscaffold : estimated apparent density
  - thermoplastic (PEEK CF30): from datasheet
  - Typical aluminum alloys used for aircraft : $\rho \sim 2.7$ g/cm³

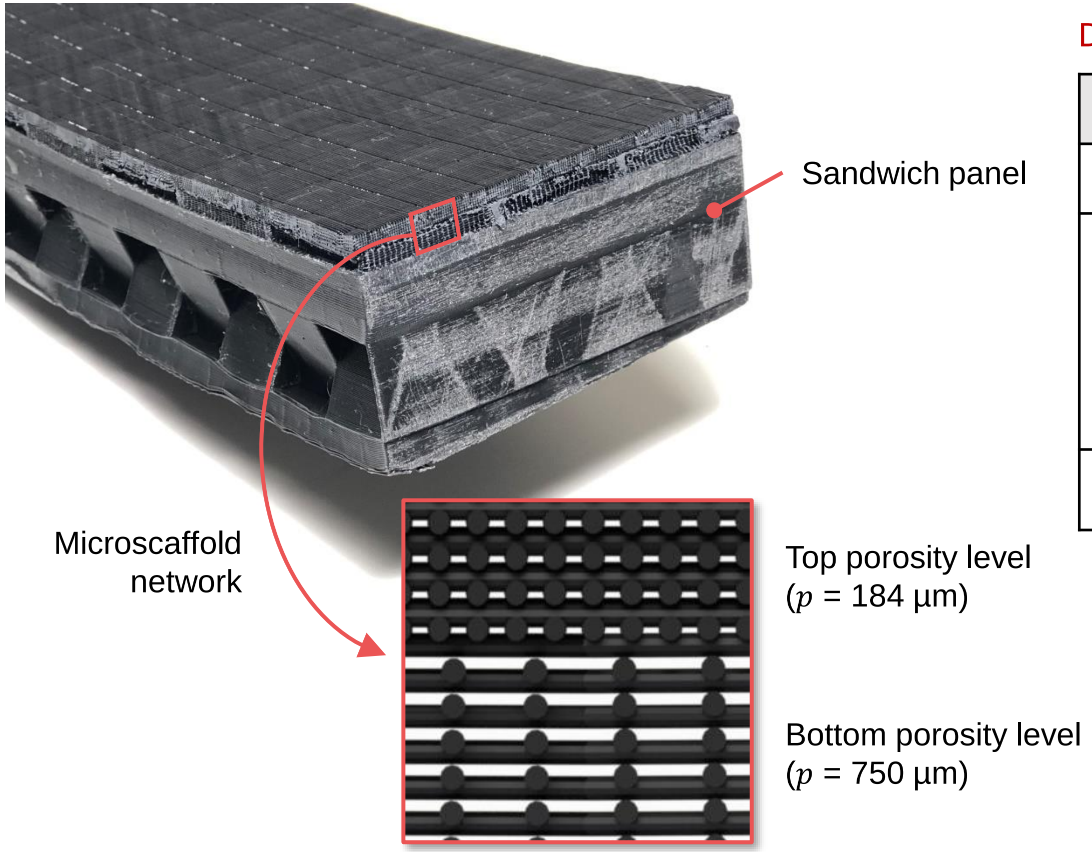

Density of benchmark and parts of the aircraft component demonstrator

Part	p (µm)	Density ρ (g/cm³)
Benchmark material (commercial EC-3524)	-	**0.505**
Abradable printable formulation	-	1.279
Bottom porosity level	750	0.346
Top porosity level	184	0.735
Overall microscaffold (both levels)	750, 184	**0.535**
PEEK CF30 material (sandwich panel)	-	**1.380**

1. In collaboration with Iee Lee Hia

MICROSCAFFOLD APPARENT DENSITY

1. Estimate the mass of each porosity level
   - Multiply the abradable formulation bulk density (1.279 g/cm³) to volumed of printed filaments
2. Divided the estimated mass by overall volume occupied by the microscaffold network

Multinozzle printhead		
α	26	nozzles
d	0.25	mm
A	0.049	mm²

overall dimensions		Unit
L	520	mm
l	78	mm
t	5.6	mm
vol	227136	mm³
	227.1	cm³

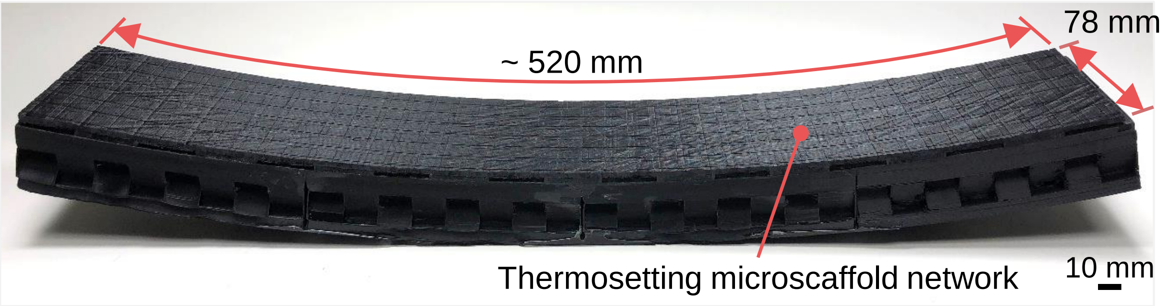

level 1	p750							
nb layers	16							
	nb pass	nb fila/layer	nb fila tot	long (mm)	vol (mm³)			
rows	19	494	3952	78	15131			
cols	3	78	624	520	15928			
thick	2.83	mm	4576		31059	mm³	31.1	cm³
vol eff	114785	mm³			14%	du vol tot	39.7	g
	114.8	cm³					0.346	g/cm³

level 2	p184							
nb layers	14							
	nb pass	nb fila/layer	nb fila tot	long (mm)	vol (mm³)			
rows	45	1170	8190	78	31358			
cols	7	182	1274	520	32519			
thick	2.74	mm	9464		63877	mm³	63.9	cm³
vol eff	111134	mm³			28%	du vol tot	81.7	g
	111.1	cm³					0.735	g/cm³

Level 1 + 2		Vol tot	94937	mm³
Nb filaments tot	14040		94.9	cm³
		Masse tot	121.4	g
		apparent density	0.535	g/cm³
		(level avg)	0.541	g/cm³
		error	1.1%	

MULTIFUNCTIONAL POTENTIAL

- Abradability characterization[1]

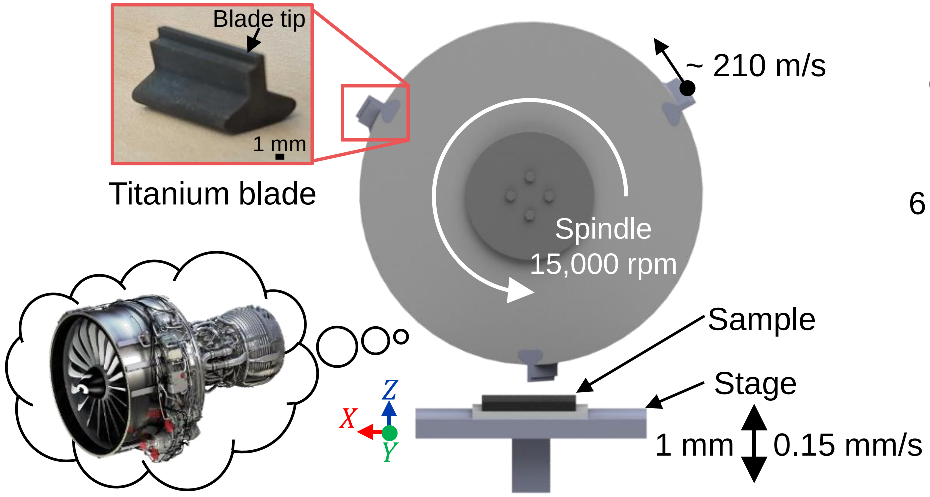

Experimental setup of the **abradability test** mimicking an engine (Safran, France).

Molded benchmark samples using hand spatula.

+

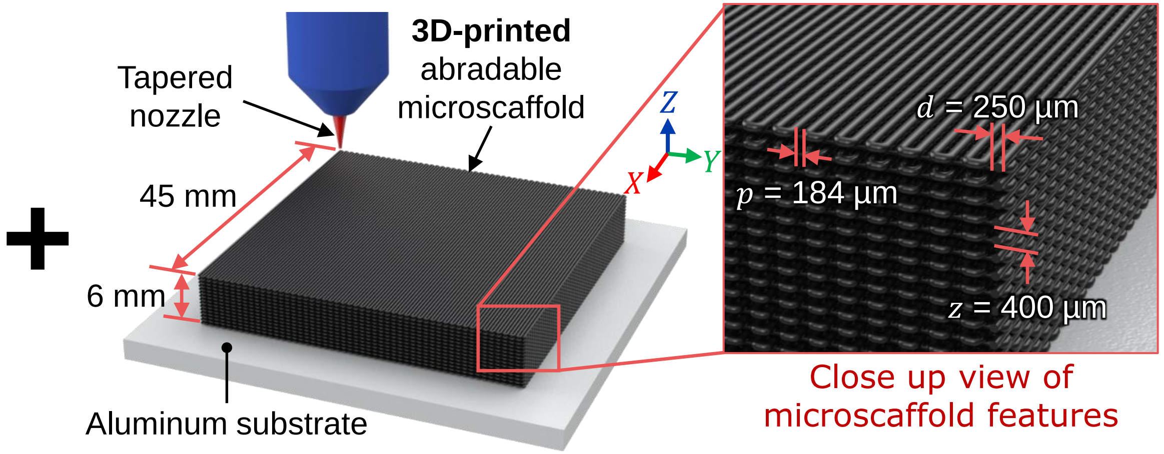

3D-printed samples using single nozzle. v **= 80 mm/s**, ΔP = 2.7 – 5.10 MPa, **30 min**.

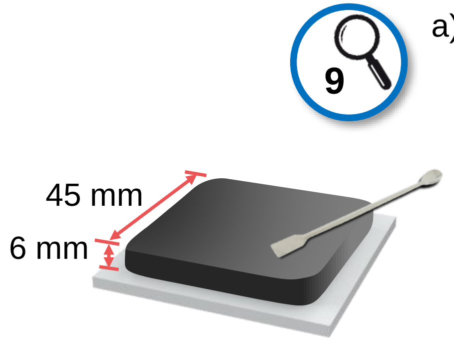

a)

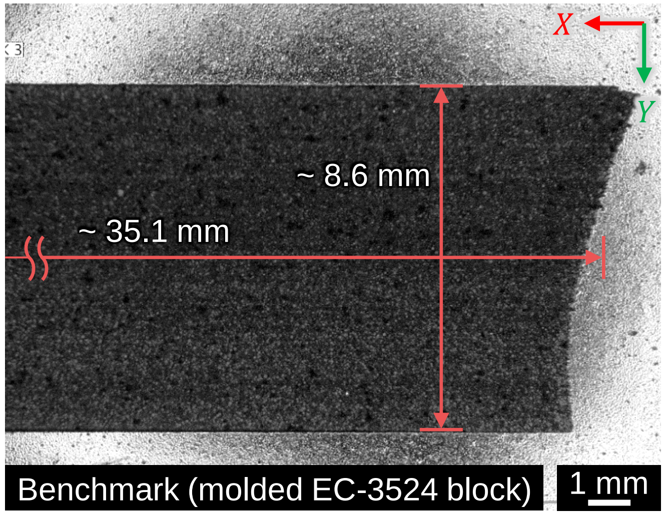

b)

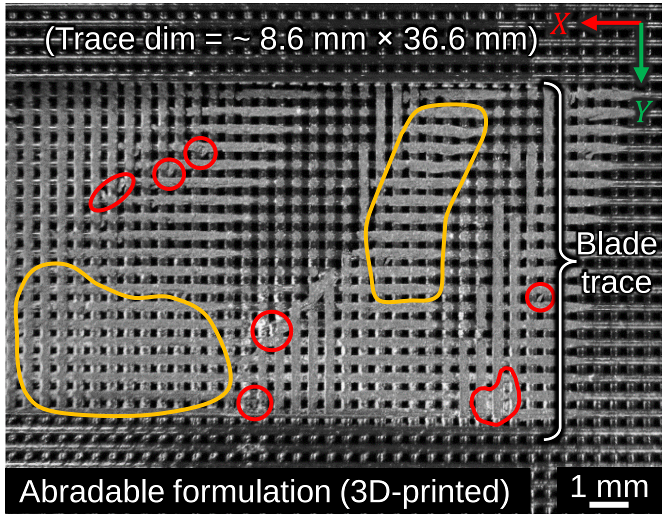

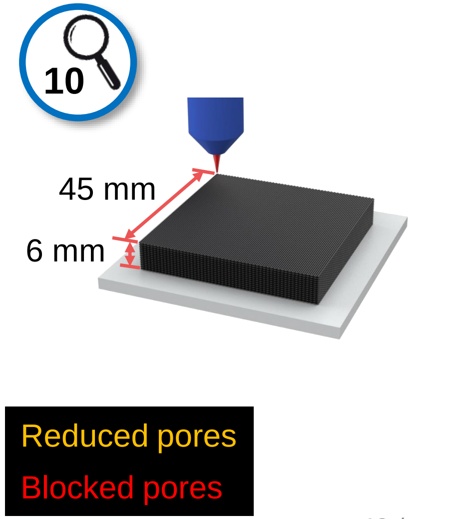

1. In collaboration with Iee Lee Hia (at Safran Aircraft Engines)

MULTIFUNCTIONAL POTENTIAL

- Abradability characterization[1]

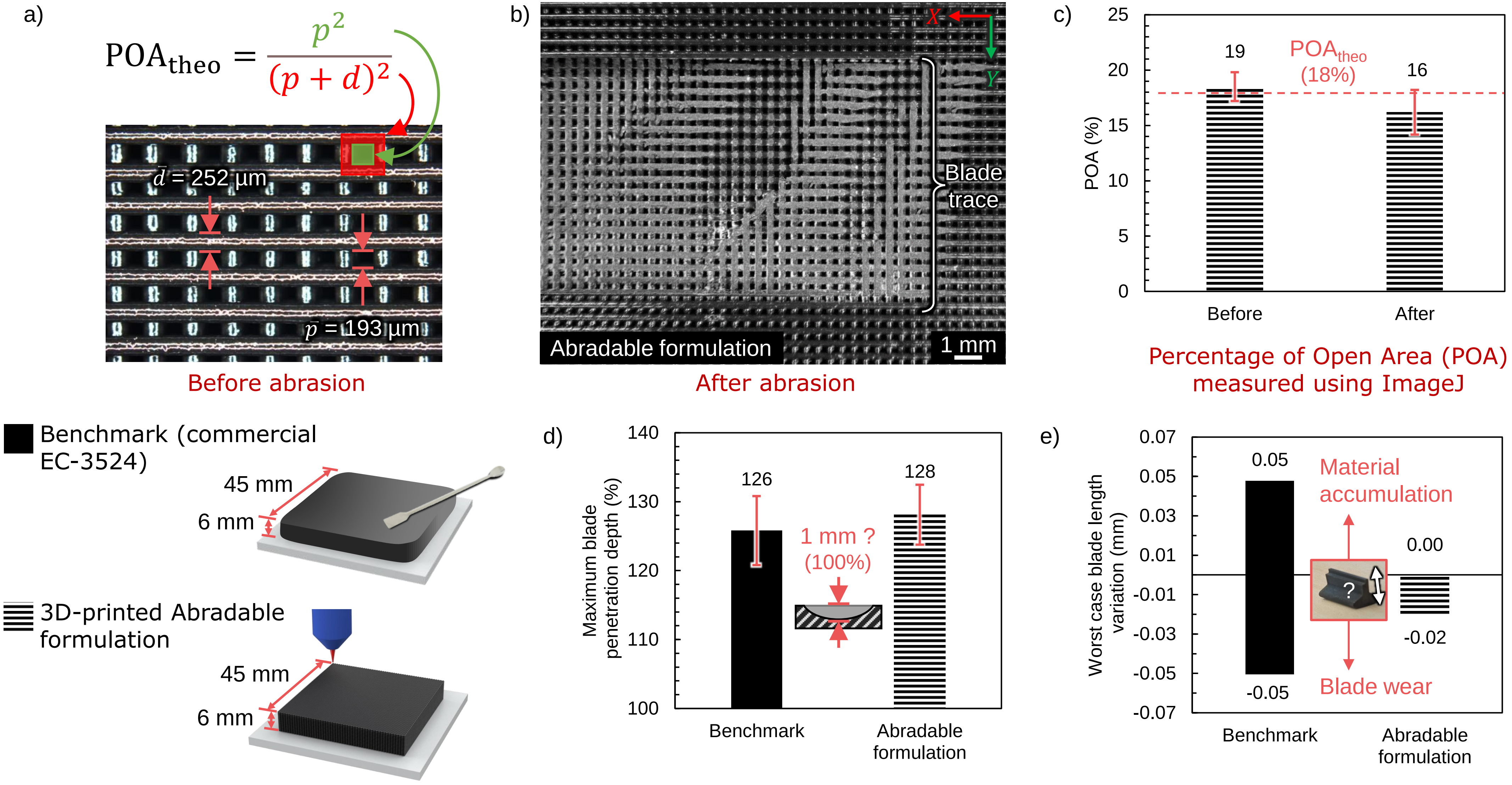

1. In collaboration with Iee Lee Hia (at Safran Aircraft Engines)